Arch. Mech., 43, 4, pp. 453–498, Warszawa 1991

An overview of boundary integral formulations for potential flows in fluid-fluid systems

E. CANOT and J.-L. ACHARD (GRENOBLE)

THE MOTION of two incompressible, constant-density fluids, separated by a moving interface is considered in a three-dimensional space without any solid boundary. In the framework of the irrotational approximation, the velocity fields are simultaneously induced either by a dipole or by a vortex distribution on the interface. In each case, the strength of the singularities obey a Fredholm integral equation of the second kind, which is solved at each time-step. Two classes of method, established by BAKER, MEIRON and ORSZAG [4] and by ROBERTS [43] respectively, are presented and compared together in their full generality. The second method appears as the simplest to deal with three-dimensional as well as axisymmetric problems. A numerical implementation of this method for axisymmetric flows has been first of all applied as a test on small vibrations of a spherical globule and then has been used to the study of the Rayleigh–Taylor instability. The nonlinear large-amplitude motion exhibits the well known dissymmetric behaviour between perturbations growing upwards (bubble) and downwards (spike), together with the development of strong shape singularities of the interface ("roll-up" and "cusp" formations).

1. Introduction

IN TWO-PHASE or two-component flows of Newtonian and incompressible fluids the existence of deformable and moving interfaces gives rise to complex free-boundary value problems. Except for turbulence effects, the mathematical formulation of these problems does not create difficulties thanks to the progress made in the description of the interfaces. Unfortunately, overwhelming obstacles occur in numerical solution (not to mention the analytical approaches which are limited to linear or quasi-nonlinear dynamics of interface) of the problems in their full generality. To obtain a solution, two classes of restrictions have been commonly used, often simultaneously. Systems which are considered possess a simple interfacial geometry as in the cases of rising bubbles, expanding or collapsing vapour cavities, oscillating droplets, or in the cases of film or separated flows. The second class introduces approximations in the equations themselves: basically the creeping flows or irrotational flows approximations.

This paper deals with various fluid-fluid systems formulations within the latter approximation. Even in this case, the computational efforts remain considerable. As severe non-linearities occur in the problem, accurate numerical methods are required, involving interface tracking schemes, in order to simulate the motion of both fluids interacting through a possibly distorted interface shape. For example, finite-difference techniques (PLESSET, CHAPMAN [38], PROSPERETTI, JACOBS [40]), marker-and-cell techniques (DALY [14]; MITCHELL, HAMMITT [34]) vortex-in-cell techniques (TRYGGVASON [51], ZUFIRIA [53]), conformal mapping methods (MENIKOFF, ZEMACH [32]) have proved their efficiency in a number of problems. Finite-element methods may also be envisaged but, generally, they are not well adapted to unsteady free-boundary problems, because their application requires the time-consuming generation of a new grid over the whole computational domain at each time-step. All these grid methods are expensive and are limited in their ability to resolve curved interfaces; it would be desirable to have a relatively inexpen-

sive, purely Lagrangian method. This has been done by developing the boundary integral method.

The boundary integral method is now firmly established as an important alternative technique to most of the methods of analysis for potential problems in fluid mechanics. This technique consists primarily in the transformation of the partial differential equations describing the behaviour of the unknown function inside and on the boundary of the domain into an integral equation relating new variables only over the boundaries. Consequently, its numerical implementation leads to drastic reduction in calculation time because the dimensionality of the effective space is reduced by one. This preliminary analytical treatment of equations which makes new variables, i.e. surface singularities, come into view, provides in itself a new insight into the physics. An outline of numerical techniques available in the literature concerning the numerical approximations of such integral equations can be found elsewhere (BAKER, MILLER [6]).

The aim of this paper is basically to present an overview of boundary integral formulations. At the beginning, integral methods were applied to steady problems, such as potential flow about solid bodies (HESS, SMITH [20]), research which took place in aeronautics and hydrodynamics. Transient problems were also taken into consideration later, and the works of LENOIR [26], BLAKE, GIBSON [8], PROSPERETTI [39] and some others are concerned with the growth or the collapse of cavitation bubbles near rigid boundaries or near a free surface. A Lagrangian description for a specified number of points on the bubble surface is used to represent the motion of the bubble, and the time-stepping procedure uses the Bernoulli pressure condition. It must be noticed that these transient models approximate the correct normal momentum balance at the interface by introducing a uniform pressure condition within the bubble. This approximation is valid if the density ratio is negligible and if the velocity scales of each phase are of about the same order. If not, this free-surface approximation no longer holds and another model must be used.

On the other side, the boundary integral formulation has been applied by BIRKHOFF [7] for an evolving vortex-sheet in a constant density fluid. In this case the vortex-sheet models a sharp discontinuity of the velocity field and not a two-phase system interface. The method of Birkhoff leads to an integro-differential equation for the position of the vortex-sheet, via a parametrization employing a circulation coordinate. But this formulation is valid only for two-dimensional problems since it is based on the theory of functions of complex variables. It has been used by a number of authors (MOORE [37], PULLIN [41], KRASNY [24]).

Our primary concern here is the description of fluid-fluid systems, where both homogeneous fluids are separated by a "phase interface" which is a region in which the properties differ from those of the adjoining fluid. Fluids may just be different and immiscible, or be identical but differ by their physical state (phase) or may also differ through a sharp transition in the concentration of a given solute. Within the framework of irrotational approximations the basic property which can jump from one side to another is the density, and the interfacial property attributable to the interface itself is possibly the surface tension. Such a restricted model is nevertheless more general than a free-surface or a vortex-sheet. BAKER, MEIRON, ORSZAG (referred to from now on as BMO) [3] (and also [4]) were the first ones to derive an integral formulation for such a "density" interface, and their method appears to be an extension of the classical "point-vortex method" which has been already used by Rosenhead in 1931 for a crude description of a vortex-sheet motion.

An alternative boundary integral formulation, where the velocity field is induced by dipole or vortex distributions, was proposed by ROBERTS [43] to solve the two-dimensional motion of a density interface; this method appears as an extension of some methods used in free-surface flow, that we shall term "Bernoulli's methods" because they use directly the Bernoulli equation for the progression in time (PLESSET, CHAPMAN [38], BLAKE *et al.* [9], LUNGREN, MANSOUR [29]). These two kinds of methods are established only for two-dimensional configuration, and in this latter case on essential differences can be found, except perhaps those concerning stability or accuracy. However, we intend to demonstrate the simplicity of the Roberts method compared to the BMO 82's one if we want to deal with axisymmetric or fully three-dimensional configurations. For this reason the two methods are re-derived in the three-dimensional case in their full generality, and the application given at the end corresponds to the axisymmetric Rayleigh–Taylor instability in an unbounded space, taking into account gravity, inertia forces and surface tension.

In the next section we present some geometrical and kinematical considerations. The equations is then reformulated in terms of the velocity potentials in each fluid. The mathematical aspects of the boundary integral formulation of the fluid-fluid systems are presented in Sect. 4. Following this, the two classes of integral formulations are developed and compared in Sect. 5. In Sect. 6, the method is first applied to the linear oscillations of a spherical globule, and then to the Rayleigh–Taylor instability; the results of the numerical simulations are discussed. The final section summarizes the main conclusions that may be drawn from this study and identifies the possible areas of future studies.

2. Geometrical and kinematical preliminaries

We will limit ourselves in this paper to two-phase systems with rigid walls rejected at infinity. Wall effects at a finite distance, including the case where the fluid interface intersects a solid boundary, will be addressed in a subsequent paper. Such systems occupy the whole three-dimensional Euclidean space $\mathcal{E}$. The two phases themselves occupy two

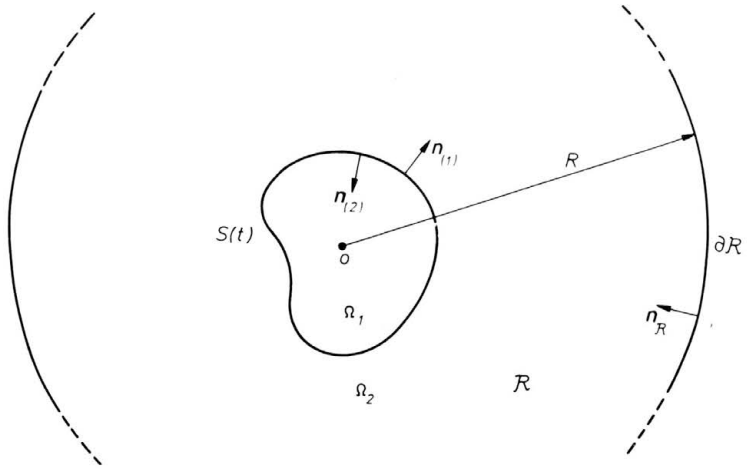

FIG. 1. Definition sketch for Case 1. The unit normal vector on $S(t)$ is directed outwards with respect to Ω_1. The unit normal vector to $\partial\mathcal{R}$ is directed inwards.

open regions $\Omega_1(t)$ and $\Omega_2(t)$; there lie on two sides of a common interfacial region which is modelled here, as usually, by a singular or dividing surface $S(t)$. Two elementary subcases are of interest. In the first one (Fig. 1), the surface $S(t)$ is a closed regular surface, Ω_1 (resp. Ω_2) being the region inside (resp. outside) the surface. In the second one (Fig. 2), the surface $S(t)$ extends to infinity (its asymptotic shape will be specified later on), Ω_1 (resp. Ω_2) being the upper (resp. lower) region; for mathematical purposes, one considers at the beginning only a finite part of Ω_2, i.e. $\Omega_2(R)$, enclosed in a sphere $\mathcal{R}$ with centre at a point $\mathcal{O}$ located in Ω_1 in the first case, and near the interface in the second case. $S(t)$ intersects necessarily $\partial\mathcal{R}$ along a curve $\mathcal{C}(t)$ (which bounds a subsurface $\Sigma(t) = S(t) \cap \mathcal{R}$ of the surface $S(t)$) in the latter case, but is completely enclosed in $\mathcal{R}$ in the former; otherwise R, the sphere radius, may be varied at will and can be infinite if required. Questions concerning the definition of the various unit vectors are given in the captions of Figs. 1 and 2. For a detailed account of the differential geometry of surfaces, the interested reader is referred to the treatise by BOWEN, WANG [10], for instance.

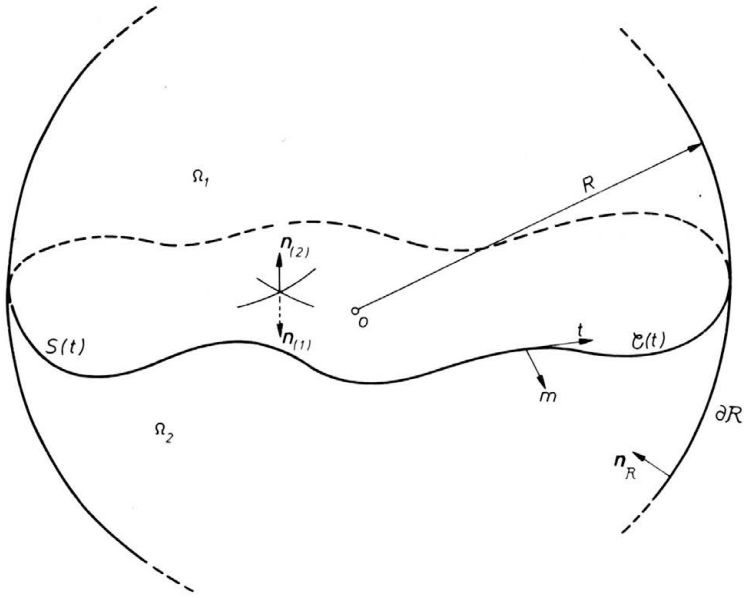

FIG. 2. Definition sketch for Case 2. The same convention is used for the unit normals to $S(t)$ and $\partial\mathcal{R}$. The unit vectors $\mathbf{t}$ and $\mathbf{m}$ lie in the plane tangent to S at $\mathcal{C}$; $\mathbf{t}$ is tangent to $\mathcal{C}$ and $\mathbf{m}$ is perpendicular to $\mathcal{C}$ and is directed outwards with respect to $\mathcal{R}$.

A moving dividing surface $S(t)$ can be viewed as a family of surfaces, one for each time t, which can be characterized either by the equation:

$$f(M,t) = 0\,, \tag{2.1}$$

where f is smooth with respect to t, and M is a point of $\mathcal{E}$, or by the smooth mapping valid at least on $\Sigma(t)$:

$$M' = M'(y^1, y^2, t)\,, \tag{2.2}$$

where (y^1, y^2) are surface coordinates. We need, moreover, in the open set $\mathcal{R}$ a coordinate system $x^i = x^i(M)$ $(i = 1, 2, 3)$, fixed in $\mathcal{E}$, to give the usual parametric representation of $\Sigma(t)$:

$$x'^i = x^i \circ M'(y^1, y^2, t) = x'^i(y^1, y^2, t), \quad i = 1, 2, 3. \tag{2.3}$$

The purpose of the present section can be stated as follows: how to generate effectively the physically or computationally convenient parametrizations $\{y^\alpha; \alpha = 1, 2\}$ of the moving surface. Actually, this problem can be split into two parts and consists of:

(i) selecting a coordinate system at time $t = 0$;

(ii) letting it evolve as the surface $\Sigma(t)$ moves in $\mathcal{R}$.

An ensuing problem is

(iii) expressing properly time-variation of physical fields defined on $\Sigma(t)$.

The first part of the problem consists then of generating coordinate systems on surfaces in $\mathcal{E}$. Indeed, this generation is not only required at time $t = 0$ but may be envisaged possibly at the end of each time step $t + dt$ and for attacking the next step from a better position. The resulting parametrization itself may be no longer adapted. Using a numerical terminology which deals with discrete entities, it can be said that the "boundary elements" on the surface (defined by the two series of evenly spaced coordinate lines in the computational plane) have to be redefined to meet several requirements, characteristic of a good mesh (or grid). These requirements are relative to the distribution of boundary elements themselves on the surface or to the distribution of "nodes" (where the unknown values are considered) which are attached to these elements. Generally speaking, it is well known that the grid employed influences greatly the accuracy of the solution. Many grid generation techniques (THOMPSON *et al.*, [50]) exist to control the placement of grid points automatically. An elementary method, which will be effectively used for the application of the present paper, is presented in Appendix 1.

The second part of the problem is devoted to following moving surface in $\mathcal{E}$. To do so, we define the velocity of the moving surface coordinate system by

$$\mathbf{w} = \left.\frac{\partial M'}{\partial t}\right|_{y^\alpha}. \tag{2.4}$$

In components related to the fixed natural basis, this velocity is written

$$w^i = \left.\frac{\partial x'^i}{\partial t}\right|_{y^\alpha}, \quad i = 1, 2, 3. \tag{2.5}$$

It can also be represented in terms of the Gauss basis $\{\mathbf{n}_{(1)}, \mathbf{a}_\alpha\}$

$$\mathbf{w} = w_n \mathbf{n}_{(1)} + w_t^\alpha \mathbf{a}_\alpha, \tag{2.6}$$

where

$$\mathbf{a}_\alpha = \frac{\partial M'}{\partial y^\alpha} \tag{2.7}$$

and it is well known that the normal component w_n, which is called the speed of displacement of the surface, does not depend on the selected system. Thus the velocity of moving surface coordinate systems will differ only by the tangential component of $\mathbf{w}$.

Three kinds of moving coordinate systems are now presented:

1. Non-drifting surface coordinate systems

A coordinate system is regarded as non-drifting on a moving surface $S(t)$ if the velocity of a constant coordinate surface point is wholly normal to the surface. Thus

$$\mathbf{w} = w_n \mathbf{n}_{(1)} . \tag{2.8}$$

We employ the notation $\{\tilde{y}^\alpha; \alpha = 1,2\}$ for this system, also called "fixed" in the surface, although this term is misleading. Non-drifting systems will be selected in our calculations because they possess interesting properties, some of them exhibited next.

2. Material surface coordinate systems

GURTIN and MURDOCH [19] define a body in sufficient generality to add the notion of a material surface S_m to the usual notion of a three-dimensional body. One of their axioms states that each material particle of S_m can be identified without ambiguity by its location in some configuration. Each material particle is thus labelled by a pair of numbers $\{y_m^\Gamma; \Gamma = 1,2\}$ corresponding to an arbitrary surface coordinate system in this configuration. The configuration may be the one of S_m at time $t = 0$ or at any time (Lagrangian point of view). Then, at each time, there exists a relation which is a diffeomorphism

$$y^\alpha = y^\alpha(y_m^1, y_m^2, t), \quad \alpha = 1,2 . \tag{2.9}$$

This relation can be viewed as giving the location (y^1, y^2) at time t of a particle (y_m^1, y_m^2). In the Lagrangian scheme, at time $t = 0$, it may reduce to the identity mapping if the reference surface coordinate system is properly chosen at that time. Instead of referring particles to surface coordinate systems, a space system of coordinates can be used by composing (2.3) with (2.9)

$$x'^i = x'^i(y_m^1, y_m^2, t), \quad i = 1,2,3 . \tag{2.10}$$

We can show here how more useful a family of non-drifting systems is. In that case we have instead of Eq. (2.9)

$$\tilde{y}^\alpha = \tilde{y}^\alpha(y_m^1, y_m^2, t), \quad \alpha = 1,2 . \tag{2.11}$$

The space velocity $\mathbf{w}$ of a material particle can be computed by using the chain derivative rule from Eqs. (2.10) and (2.11), and by virtue of (2.8)

$$\mathbf{w} = w_n \mathbf{n}_{(1)} + \left.\frac{\partial \tilde{y}^\alpha}{\partial t}\right|_{y_m^\Gamma} \tilde{\mathbf{a}}_\alpha , \tag{2.12}$$

where $\{\mathbf{n}_{(1)}, \tilde{\mathbf{a}}_\alpha\}$ is the Gauss basis relative to $\{\tilde{y}^\alpha; \alpha = 1,2\}$.

Thus

$$\left.\frac{\partial \tilde{y}^\alpha}{\partial t}\right|_{y_m^\Gamma}$$

is the α component w_t^α of the tangential velocity of the particle. On the opposite now, dealing with a general coordinate $\{y^\alpha; \alpha = 1,2\}$, the term

$$\left.\frac{\partial y^\alpha}{\partial t}\right|_{y_m^\Gamma}$$

is not equal to w_t^α since the new reference frame is itself drifting on the surface.

3. Fictitious particles' surface coordinate systems

Any transformation between surface coordinate systems such as

$$\tilde{y}^\alpha = \tilde{y}^\alpha(y_f^1, y_f^2, t), \quad \alpha = 1,2, \tag{2.13}$$

whose dependance with respect to t is assumed to be regular enough, can be considered as defining the position of fictitious particles labelled by (y_f^1, y_f^2). The occurrence of such fictitious particles may result from various physical or computational reasons; in the latter case they correspond to surface markers. Let us present two of them.

Each time when there is a mass transfer between the dividing surface and the two adjoining phases, the dividing surface is crossed by a flux of material particles and it can be no longer considered as a material surface. But, following DELHAYE [16] for instance, the fictitious particle velocity $\mathbf{w}_f$ can be defined

$$\mathbf{w}_f = w_n \mathbf{n}_{(1)} + \mathbf{w}_{ft}. \tag{2.14}$$

Its tangential part is equal to the one of $\mathbf{v}_{(1)}$ and $\mathbf{v}_{(2)}$ in either adjoining phase evaluated at $S(t)$. If we introduce the notation for the limits on each side of S:

$$\mathbf{v}_{(k)}|_S = \lim_{\substack{M \to S \\ M \in \Omega_k}} \mathbf{v}_{(k)} \tag{2.15}$$

then we have, by using the projection operator $\mathbf{P}$ (BOWEN, WANG, [10]):

$$\mathbf{w}_{ft} = \mathbf{P}(\mathbf{v}_{(1)}|_S) = \mathbf{P}(\mathbf{v}_{(2)}|_S) \tag{2.16}$$

this last statement being allowed by the usual assumption of continuity experienced by material tangential velocities through an interface. The transformation (2.13) is thus given by solving the set of equations

$$\left.\frac{\partial \tilde{y}^\alpha}{\partial t}\right|_{y_f^\Gamma} = \mathbf{w}_{ft} \cdot \tilde{\mathbf{a}}^\alpha, \quad \alpha = 1,2. \tag{2.17}$$

In the context of irrotational motions of two different immiscible fluids separated by a dividing surface, the tangential component of the velocity field always experiences a jump, whereas its normal component remains continuous. In this case, it is obvious that any average of the form

$$\mathbf{w}_l = \frac{1}{2}(\mathbf{v}_{(1)}|_S + \mathbf{v}_{(2)}|_S) + \frac{1}{2}F(\mathbf{v}_{(1)}|_S - \mathbf{v}_{(2)}|_S) \tag{2.18}$$

has its normal component which is equal to the speed of displacement of the interface w_n, and defines a new kind of fictitious particles, termed "Langrangian markers" about vortex-sheet-like formulations of interfacial motions (BMO [4]). So, their position is derived again from

$$\left.\frac{\partial \tilde{y}^\alpha}{\partial t}\right|_{y_l^\Gamma} = \mathbf{w}_{lt} \cdot \tilde{\mathbf{a}}^\alpha, \quad \alpha = 1,2. \tag{2.19}$$

The weighting factor F is in fact a continuous simple-valued function of the coordinates (y_f^1, y_f^2), and by choosing $F = 1$ or $F = -1$ the markers follow the continuous material particles in phase 1 and 2, respectively. It is usual to impose

$$-1 \leq F \leq 1,$$

and it may be convenient to use the arbitrariness of F to control the position of the markers on the surface (PULLIN [41]).

Now, the basic materials allowing any physical fields to be defined on the moving surface has been presented. In this third part of this section, let us see how an observer can compute time variations of these fields, say φ for a scalar field. Two cases have to be distinguished. Either $\varphi = \varphi_k$ is defined on the contiguous k-th three-dimensional phase or $\varphi = \varphi'$ is defined only on the surface.

In the first case, one can use the classical material time derivative of $\varphi_k(x^i, t)$

$$\frac{d}{dt}\varphi_k[x^i(x_f^j, t), t] = \left.\frac{\partial \varphi_k}{\partial t}\right|_{x^i} + \left.\frac{\partial \varphi_k}{\partial x^i}\frac{\partial x^i}{\partial t}\right|_{x_f^j}, \tag{2.20}$$

where $x^i = x^i(x_f^i, t)$, $i = 1, 2$ is the diffeomorphism, analogous to Eq. (2.9) for a material surface, giving the motion of a three-dimensional body, composed of real or fictitious material particles.

The space velocity $\mathbf{v}$ of a material particle (x_f^1, x_f^2, x_f^3) is represented by

$$\mathbf{v} = \mathbf{g}_i \left.\frac{\partial x^i}{\partial t}\right|_{x_f^j}, \tag{2.21}$$

where $\{\mathbf{g}_i; i = 1, 2, 3\}$ is the natural basis of the fixed system of coordinates. Thus (2.20) can be written as

$$\frac{d\varphi_k}{dt} = \left.\frac{\partial \varphi_k}{\partial t}\right|_{x^i} + \frac{\partial \varphi_k}{\partial x^i}\mathbf{g}^j \cdot v = \frac{\partial \varphi_k}{\partial t} + \nabla \varphi_k \cdot v \tag{2.22}$$

and the limiting form of this equation on the k-th side of S is written as

$$\frac{d_s \varphi_k}{dt} = \lim_{\substack{M \to S \\ M \in \Omega_k}} \frac{d\varphi_k}{dt} = \frac{\partial \varphi_k|_S}{\partial t} + \nabla \varphi_{k|_S} \cdot w_f . \tag{2.23}$$

This expression is not convenient in the second case since $\frac{\partial \varphi'}{\partial t}|_{x^i}$ has no meaning nor does $\nabla \varphi'$. Instead of referring to a fixed system of coordinates $\{x^i;\ i = 1, 2, 3\}$ selected in $\mathcal{E}$, we can refer to a non-drifting system of coordinates $\{\tilde{y}^\alpha;\ \alpha = 1, 2\}$ selected on Σ, and instead of Eq. (2.20) we have

$$\frac{d_s}{dt}\varphi'[\tilde{y}^\alpha(y_f^\Gamma, t), t] = \left.\frac{\partial \varphi'}{\partial t}\right|_{\tilde{y}^\alpha} + \left.\frac{\partial \varphi'}{\partial \tilde{y}^\alpha}\frac{\partial \tilde{y}^\alpha}{\partial t}\right|_{y_f^\Gamma}. \tag{2.24}$$

Using Eq. (2.17), this equation becomes

$$\frac{d_s \varphi'}{dt} = \left.\frac{\partial \varphi'}{\partial t}\right|_{\tilde{y}^\alpha} + \frac{\partial \varphi'}{\partial \tilde{y}^\alpha}\mathbf{w}_{ft} \cdot \tilde{\mathbf{a}}^\alpha = \frac{\partial \varphi'}{\partial t} + \nabla_S \varphi' \cdot w_{ft}, \tag{2.25}$$

where ∇_S is the surface gradient.

Equations (2.23) and (2.25) can be generalized to the surface vector field

$$\mathbf{u}' = u_n \mathbf{n}_{(1)} + \mathbf{u}_t = \mathbf{u}'[\tilde{y}^\alpha(y_f^\Gamma, t), t].$$

It can be shown that

$$\begin{aligned} \frac{d_s}{dt}\mathbf{u}' &= \left.\frac{\partial \mathbf{u}'}{\partial t}\right|_{\tilde{y}^\alpha} + \left.\frac{\partial \mathbf{u}'}{\partial \tilde{y}^\alpha}\frac{\partial \tilde{y}^\alpha}{\partial t}\right|_{y_f^\Gamma} \\ &= \left.\frac{\partial \mathbf{u}'}{\partial t}\right|_{\tilde{y}^\alpha} + (\nabla_s \mathbf{u}_t)\mathbf{w}_{ft} + [\mathbf{w}_{ft} \cdot \mathbf{B}(\mathbf{u}_t)]\mathbf{n}_{(1)} - u_n \mathbf{B}(\mathbf{w}_{ft}) + \mathbf{n}_{(1)}\frac{\partial u_n}{\partial \tilde{y}^\alpha} w_t^\alpha . \end{aligned} \tag{2.26}$$

The operator $\mathbf{B} = -(\mathbf{P} \circ \nabla \mathbf{n}_{(1)}) = -\nabla_s \mathbf{n}_{(1)}$ is the Weingarten map, whereas the twice covariant tensor associated with $\mathbf{B}$ is the second fundamental form. It can be represented in component form by using Weingarten's formula

$$\mathbf{B} = b_{\alpha\gamma}\tilde{\mathbf{a}}^{\gamma} \otimes \tilde{\mathbf{a}}^{\alpha} = b^{\gamma}_{\alpha}\tilde{\mathbf{a}}_{\gamma} \otimes \tilde{\mathbf{a}}^{\alpha}\,. \tag{2.27}$$

A special case of interest is when $\mathbf{u}' = \mathbf{n}_{(1)}$

$$\frac{d_s \mathbf{n}_{(1)}}{dt} = \left.\frac{\partial \mathbf{n}_{(1)}}{\partial t}\right|_{\tilde{y}^{\alpha}} - \mathbf{B}(\mathbf{w}_{ft})\,, \tag{2.28}$$

where the first derivative can be written

$$\left.\frac{\partial \mathbf{n}_{(1)}}{\partial t}\right|_{\tilde{y}^{\alpha}} = -\nabla_s w_n\,. \tag{2.29}$$

Note that H the mean curvature of the surface is given by $b^{\alpha}_{\alpha}/2$.

3. Equations of motion. The potential approximation

In this section we derive the whole set of equations for the two classes of two-phase systems having geometries as in Figs. 1 and 2, when the motion of the two incompressible fluids is considered as irrotational.

The motion of the Newtonian and incompressible fluid k ($k = 1, 2$) adjacent to the interface is described by the following continuity and momentum equations:

$$\nabla \cdot \mathbf{v}_{(k)} = 0\,, \tag{3.1}$$

$$\frac{\partial \mathbf{v}_{(k)}}{\partial t} + (\nabla \mathbf{v}_{(k)})\mathbf{v}_{(k)} = \mathbf{F} - \frac{1}{\varrho_k}\nabla p_k + \frac{\mu_k}{\varrho_k}\Delta \mathbf{v}_{(k)}\,, \tag{3.2}$$

where $\mathbf{v}_{(k)}$ and p_k are the velocity and pressure fields, ϱ_k, μ_k are the constant density, dynamic viscosity, $\mathbf{F}$ is the body force per unit mass, and Δ is the vector Laplacian. Describing now the general boundary conditions in both classes of topological systems considered at the beginning, we have

$$\mathbf{v}_{(k)} \to 0 \quad \text{as} \quad r \to \infty\,, \tag{3.3}$$

where $r = |\mathrm{OM}|$ for the fluids which extend to infinity. Moreover, for three-dimensional flow extending to infinity, it is well known that $\mathbf{v}_{(k)}$ has the asymptotic form

$$\mathbf{v}_{(k)} = O\left(\frac{1}{r^3}\right) \quad \text{as} \quad r \to \infty\,. \tag{3.4}$$

The above partial differential equations valid in Ω_k and boundary conditions must be supplemented by appropriate jump conditions valid on the dividing surface representing the effects of the interfacial region. There is nowadays a general agreement (SLATTERY and FLUMERFELT, [46]) concerning the derivation of general conservation laws valid at each position on this surface. Recall that our problem is to define well-posed purely irrotational models from this whole set of exact equations: the non-slip condition and the tangential component of the momentum balance must be left aside. If, moreover, there is no mass transfer across the dividing surface, we only need the continuity of normal velocities

$$\mathbf{v}_{(1)} \cdot \mathbf{n}_{(1)} = -\mathbf{v}_{(2)} \cdot \mathbf{n}_{(2)}\,, \tag{3.5}$$

while the normal momentum balance reduces, if H denotes the mean curvature of the surface and T the surface tension, to

$$2HT + (p_1 - p_2)|_s - 2[\mu_1(\mathbf{n}_{(1)} \cdot \nabla \mathbf{v}_{(1)}) \cdot \mathbf{n}_{(1)} - \mu_2(\mathbf{n}_{(2)} \cdot \nabla \mathbf{v}_{(2)}) \cdot \mathbf{n}_{(2)}] = 0, \tag{3.6}$$

in which, due to viscosity, remains a normal stress component. This term, the only one which creates dissipation, has been taken into consideration by several authors (MOORE [35], CESCHIA, NABERGOJ [12], KANG, LEAL [22]). Besides, more refined works including viscous effects have been undertaken (MOORE [36], MIKSIS *et al.* [33], LUNDGREN, MANSOUR [29]). Corrections of pressure field in the vicinity of the interface are made by retaining first-order viscous terms in the normal stress boundary condition. The calculation of this first-order correction is always based on previous calculation of the potential flow. In our case, as we are restricted to motions of two inviscid fluids, the last term in Eq. (3.6) disappears. Finally, these boundary conditions must be completed by the initial conditions

$$\mathbf{v}_{(k)} = \mathbf{v}_{(k),0} \quad \text{at} \quad t = 0, \quad k = 1, 2. \tag{3.7}$$

The resulting equations can now be listed, expressed in terms of the scalar potentials φ_k. The continuity equation (3.1) gives

$$\nabla^2 \varphi_k = 0, \quad k = 1, 2, \tag{3.8}$$

whereas the momentum equations (3.2) can be integrated, giving the Bernoulli equations

$$\frac{\partial \varphi_k}{\partial t} + \frac{1}{2}\mathbf{v}_{(k)}^2 + \psi_k + \frac{1}{\varrho_k} p_k = 0, \quad k = 1, 2. \tag{3.9}$$

In Case 2, where the two fluids extend to infinity, the constants of integration in (3.9) vanish due to the asymptotic behaviour

$$\varphi_k \to 0 \quad \text{as} \quad r \to \infty \tag{3.10}$$

or, more precisely thanks to Eq. (3.4),

$$\varphi_k = O\left(\frac{1}{r^2}\right) \quad \text{as} \quad r \to \infty, \tag{3.11}$$

and due to the choice of the potential energy per unit mass ψ_k associated with the field $\mathbf{F}$, which are uniquely defined by the following asymptotic behaviour

$$p_k + \varrho_k \psi_k \to 0 \quad \text{as} \quad r \to \infty. \tag{3.12}$$

In Case 1, the procedure holds again for fluid $k = 2$, whereas Eq. (3.9) is verified for fluid $k = 1$ because φ_1 is defined up to an additive constant.

The two scalar fields φ_k are coupled at the interface by the following Neumann condition, coming from Eq. (3.5)

$$\mathbf{n}_{(1)} \cdot \nabla \varphi_1|_S + \mathbf{n}_{(2)} \cdot \nabla \varphi_2|_S = 0. \tag{3.13}$$

The normal momentum balance at the interface (3.6) becomes

$$(p_1 - p_2)|_S + 2HT = 0. \tag{3.14}$$

In this paper, $\mathbf{F}$ corresponds to a uniform gravitational field, so

$$\psi_1 - \psi_2 = Cte = \Psi. \tag{3.15}$$

Of course, the initial conditions must be added to this new system of equations, and (3.7) takes the form

$$\varphi_{(k)} = \varphi_{(k),0} \quad \text{at} \quad t = 0 \quad (k = 1, 2). \tag{3.16}$$

Let us examine a particular case which occurs for gas-liquid systems. In such a case, we have $\varrho_1 \ll \varrho_2$, when the gas occupies the domain Ω_1, and the liquid Ω_2. So, the usual constant pressure condition can be derived from Eq. (3.9)

$$p_1 = C^{te} \quad \text{in} \quad \Omega_1 . \tag{3.17}$$

This approximation, which is the so-called "free-surface condition", considers the gas as a passive, or dynamically inactive medium. But it is valid if and only if the velocity scales of each phase are of the same order.

4. Integral formulations

4.1. Mathematical background and general features

In this section, we present some basic results of the potential theory about superficial distributions of singularities. Recalled for the case of a single-phase flow, these properties are extended for two-phase flow systems.

Classical potential theory shows, as is well known (STAKGOLD [47]), that the potential of an irrotational single-phase flow, impressed by rigid boundaries S_w, in a region Ω interior or exterior to S_w, may be generated by distributions of appropriate singularities (sources and/or doublets) spread over S_w. In two-phase flow systems we shall see that similar representations hold, the singularities being spread over the dividing surface. It happens moreover that these singularity layers are able to generate simultaneously irrotational flows in both phases. To understand how the "single phase" boundary integral method can be extended to cope with two-phase systems, consider for definiteness the standard interior Dirichlet problem. Of course, in the field of hydrodynamics we are generally faced with interior or exterior problems of the Neumann type; since they have some extra critical mathematical features, they will be addressed as applications in a second step.

In the following, we are restricted to the Case 1, and we study solutions to Laplace's equation

$$\nabla^2 \varphi_1 = 0 \quad \text{in} \quad \Omega_1 , \tag{4.1}$$

with boundary conditions of the Dirichlet type

$$\varphi_1|_S = \varphi_S , \tag{4.2}$$

where φ_S are prescribed values of the function over the boundary S. Now we attempt to find the solution of Eqs. (4.1) and (4.2) in the form of a sum of a single-layer potential and a double-layer potential spread on S

$$\varphi_1(M) = -\int_S [\sigma(M')G(M, M') + \tau(M')\nabla' G(M, M') \cdot \mathbf{n}(M')]\, dS' , \tag{4.3}$$

where $\mathbf{n}$ is the unit outward normal on S, $G(M, M')$ is the fundamental solution to Laplace's equation; σ is the strength of the surface source distribution (charge in electrostatics); τ is the strength of the surface doublet with normal axis distribution (dipole in electrostatics). The fundamental solution $G(M, M')$ is also known as the Newtonian

potential for 3-D problems or the logarithmic potential for 2-D problems. As we are restricted to the former, we have

$$G(M, M') = \frac{1}{4\pi s}, \tag{4.4}$$

where $s = |MM'|$ is the distance between the observation point M and the singularity point M'.∇' (resp. ∇) refers to the gradient with respect to the variable M' (resp. M). It is clear that any single layer and double layer potentials are harmonic in Ω_1 and so does φ_1 as given by Eq. (4.3). Such a function will be a solution of Eqs. (4.1) and (4.2) if the distribution strengths σ and τ are adjusted to satisfy the boundary condition (4.2). To impose these constraints we have to know the behaviour of the potential Eq. (4.3) as the observation point M is taken to a boundary point P from inside Ω_1.

The LHS of Eq. (4.3) is then from Eq. (4.2)

$$\lim_{\substack{M \to P \\ M \in \Omega_1}} \varphi_1(M) = \varphi_1(P)|_S = \varphi_S . \tag{4.5}$$

Performing the same limiting process it is well known that the potential of a simple layer is continuous and the first integral approaches

$$-\int_S \sigma(M')G(P, M')\, dS' . \tag{4.6}$$

Finally, the potential of a double layer experiences a discontinuity upon crossing the layer and the second integral becomes

$$\frac{1}{2}\tau(P) - \int_S \tau(M')\nabla' G(P, M') \cdot \mathbf{n}(M')\, dS' . \tag{4.7}$$

According to Eqs. (4.2) (4.3) and (4.5), σ and τ must be a solution of the equation

$$\varphi_S(P) = \frac{1}{2}\tau(P) - \int_S \sigma(M')G(P, M')\, dS' - \int_S \tau(M')\nabla' G(P, M') \cdot n(M')\, dS' . \tag{4.8}$$

Since there is only one constraint and there are two unknowns σ and τ, there is a degree of freedom in the problem. To make the boundary integral representation unique, we have to introduce auxiliary conditions. These conditions, that we shall call "singularity selection rules", may lead to representations which are more simple numerically, or more illuminating physically or more convenient mathematically. We are going to show that every rule, of whatever suitability, can be viewed as a way, which remains generally implicit, of specifying simultaneously, via (σ, τ), a fictitious harmonic potential field in the complementary part of the region of interest. The advantage of such a point of view is two-fold:

(i) The so called "direct" and "indirect" formulations of the boundary element method (BREBBIA *et al.*, [11]) can be encompassed within a unified frame.

(ii) It suggests a straightforward extension for the description of two-phase systems.

Indeed, let us assume that we have found a couple of solutions (σ, τ) such that the representation (4.3) satisfies the interior Dirichlet problem (4.1), (4.2). Simultaneously such a representation induces outside Ω_1 harmonic potential field which has no physical relevance and that we call fictitious. Conversely, assume a fictitious problem to be given

(of the Dirichlet, Neumann or whatsoever type); if we require that the representation (4.3) satisfies both problems then no indetermination remains. To support these statements we need some basic functional relation on the surface that is going to be derived under a general hypothesis, i.e. by requiring only φ_1 to be harmonic.

Simultaneously with Eq. (4.1) we shall consider the harmonic problem

$$\nabla^2\varphi_2 = 0 \quad \text{in} \quad \Omega_2 \tag{4.9}$$

with boundary condition at infinity of the Dirichlet type

$$\varphi_2|_\infty = 0\,. \tag{4.10}$$

The boundary condition on S is left unspecified for the moment, except that we have the properties

$$\left.\begin{aligned} \varphi_2 &= O\left(\frac{1}{r^2}\right) \\ \frac{\partial\varphi_2}{\partial r} &= O\left(\frac{1}{r^3}\right) \end{aligned}\right\} \quad \text{as} \quad r \to \infty\,. \tag{4.11}$$

Let us apply Green's third identity on Ω_1 with the function φ_1

$$E_1(M)\varphi_1(M) = \int_S \mathbf{n}(M')\cdot[G(M,M')\nabla'\varphi_1 - \varphi_1\nabla'G(M,M')]\,dS'\,, \tag{4.12}$$

where

$$E_1(M) = 1 - \frac{\alpha_1(M)}{4\pi} \tag{4.13}$$

with α_1 being the solid angle described by the boundary of Ω_1 as seen by an observer at M. Namely, $E_1 = 1$ inside Ω_1, $E_1 = 0$ outside and $E_1 = 1/2$ on a smooth point of S, i.e. on all points of S.

Similarly, let us apply the same identity over $\Omega_2(R)$, bounded internally by S and externally by the surface $\partial\mathcal{R}$, with the function φ_2

$$\begin{aligned} E_2(M)\varphi_2(M) = &-\int_S \mathbf{n}(M')\cdot[G(M,M')\nabla'\varphi_2 - \varphi_2\nabla'G(M,M')]\,dS' \\ &+ \int_{\partial\mathcal{R}} \mathbf{n}_{(R)}(M')\cdot[G(M,M')\nabla'\varphi_2 - \varphi_2\nabla'G(M,M')]\,dS'\,, \end{aligned} \tag{4.14}$$

where

$$E_2(M) = 1 - \frac{\alpha_2(M)}{4\pi}\,, \tag{4.15}$$

with α_2 being the solid angle described by the boundary of $\Omega_2(R)$ as seen by an observer at M. Namely, $E_2 = 1$ inside $\Omega_2(R)$, $E_2 = 0$ outside and $E_2 = 1/2$ on S and on $\partial\mathcal{R}$.

By using the estimates (4.11) and by remarking that, M being fixed,

$$\left.\begin{aligned} G(M,M') &= O\left(\frac{1}{R}\right)\,, \\ \frac{\partial G}{\partial R}(M,M') &= O\left(\frac{1}{R^2}\right)\,, \end{aligned}\right. \tag{4.16}$$

uniformly as $R \to \infty$, we note that the contribution from the sphere vanishes as $R \to \infty$.

We now add Eq. (4.12) and the limiting form of Eq. (4.14) when $R \to \infty$

$$(4.17)\quad \varphi(M) = \begin{cases} \varphi_1 & \text{if } M \in \Omega_1 \\ \frac{1}{2}(\varphi_1 + \varphi_2) & \text{if } M \in S \\ \varphi_2 & \text{if } M \in \Omega_2 \end{cases}$$

$$= \int_S \mathbf{n}(M') \cdot [G(M, M')\nabla'(\varphi_1 - \varphi_2) - (\varphi_1 - \varphi_2)\nabla' G(M, M')]\, dS' .$$

Comparing Eqs. (4.3) and (4.17) we find

$$(4.18)\quad \sigma = -\mathbf{n}_{(1)} \cdot [\nabla(\varphi_1 - \varphi_2)]|_S ,$$

$$(4.19)\quad \tau = (\varphi_1 - \varphi_2)|_S .$$

By using similar arguments (i.e. by using the sphere $\mathcal{R}$ as a transitional object), a functional relation which is formally identical with (4.17) can be obtained for the Case 2. In this case when $R \to \infty$, $\Sigma(t) \to S(t)$ and the integral is extended over an infinite surface.

Now we are in a position to show that all classical selection rules correspond in achieving the definition of the exterior problem (4.9) and (4.10).

4.2. The classical indirect formulation

In the classical approach, we assume that the unknown function φ_1 may be expressed solely as a double layer potential with unknown strength τ. Equivalently, we may require the fictitious problem (4.9) to be of a Neumann type, since we know that φ_1 can be found uniquely on S

$$(4.20)\quad \sigma = 0 = -\mathbf{n}_{(1)} \cdot [\nabla(\varphi_1 - \varphi_2)]|_S .$$

Combining (4.17) with (4.2) and by use of (4.19) and (4.20), we obtain a Fredholm equation of the second kind

$$(4.21)\quad \varphi_S(P) = \frac{1}{2}\tau(P) - \int_S \tau(M')\nabla' G(P, M') \cdot n(M')\, dS' .$$

Regarding the numerical solution of Eq. (4.21) which corresponds to algebraic equations obtained by discretization, the presence of the term outside the integral, characteristic of Fredholm integral equations of the second kind, ensures diagonal dominance in the system matrix (BREBBIA *et al.*, [11]). The problem being well conditioned, this formulation has been extensively used. For definiteness, the interior problem will be considered again as of the Dirichlet type; similar conclusions could have been drawn for an interior Neumann problem.

4.3. The second indirect formulation

Here we assume that the unknown function φ_1 may be expressed solely as a single-layer potential with unknown strength σ. Equivalently, we may require the fictitious problem (4.9) to be a Dirichlet type, since we know that φ_1 can be found uniquely on S

$$(4.22)\quad \tau = 0 = (\varphi_1 - \varphi_2)|_S .$$

Combining Eqs. (4.17) and (4.2), and then using of (4.18) and (4.22), we obtain a Fredholm equation of the first kind

$$\varphi_S(P) = -\int_S \sigma(M')G(P, M')\,dS' . \tag{4.23}$$

A Fredholm equation of the first kind with a non-singular kernel is ill conditioned and very difficult to solve. However, in this case, the singular kernel ensures diagonal dominance in the system matrix (JASWON and SYMM [21]).

4.4. The direct formulation

Here we require trivially

$$\varphi_2|_S = \mathbf{n}_{(1)} \cdot [\nabla\varphi_2]|_S = 0 . \tag{4.24}$$

The fictitious potential is everywhere on Ω_2 equal to zero and Eq. (4.17) becomes

$$\begin{cases} \varphi_1 & \text{if } M \in \Omega_1 \\ \frac{1}{2}\varphi_1 & \text{if } M \in S \\ 0 & \text{if } M \in \Omega_2 \end{cases} = \int_S \mathbf{n}(M') \cdot [G(M, M')\nabla'\varphi_1|_S - \varphi_1|_S \nabla' G(M, M')]\,dS' . \tag{4.25}$$

This equation represents a functional constraint between the Dirichlet boundary conditions (φ_1 defined) and the Neumann boundary conditions ($\mathbf{n} \cdot \nabla'\varphi_1$ defined). Since here we are restricted to the former, Eq. (4.25) becomes a Fredholm equation of the first kind for the unknown boundary values of $\mathbf{n} \cdot \nabla'\varphi_1$.

As the unknowns in the integral equation (4.25) are physical quantities (either φ_1 or $\mathbf{n} \cdot \nabla'\varphi_1$), this formulation is said to be direct to distinguish it for instance from formulations (1) and (2) that involve strengths σ and τ of "fictitious" singularities. These latter singularities are not less physical, from our point of view, than the ones arising in the former formulation: all of them correspond to an arbitrary choice in defining the complementary problem. What is true is that in this formulation (3) we obtain directly the non-specified boundary data (i.e. $\mathbf{n} \cdot \nabla'\varphi_1$) after the source density distribution has been found.

4.5. Adequate formulation for fluid-fluid systems

The key to the extension of the above boundary integral methods to fluid-fluid systems is to turn the basic underdetermination of its initial formulation to account. The flow of one of the phases being considered, we require the complementary flow to be just the flow of the other phase. To put it in another way, we require the representation (4.17) to satisfy at once the problems for the potential flows in each phase region and on the dividing surface. The starting point is the functional relation which has been derived under fairly general conditions, i.e. Eqs. (4.1), (4.9) and (4.10), for both Cases 1 and 2. Its expression is the same for these two cases, except that in Case 2, the surface S extends to infinity.

$$\begin{cases} \varphi_1 & \text{if } M \in \Omega_1 \\ \frac{1}{2}(\varphi_1 + \varphi_2) & \text{if } M \in S \\ \varphi_2 & \text{if } M \in \Omega_2 \end{cases} = \int_S \mathbf{n}(M') \cdot [G(M, M')\nabla'(\varphi_1 - \varphi_2)|_S - (\varphi_1 - \varphi_2)|_S \nabla' G(M, M')]\,dS' . \tag{4.26}$$

Using the interfacial condition (3.13) which is equivalent to

$$\mathbf{n} \cdot \nabla'(\varphi_1 - \varphi_2) = 0\,, \tag{4.27}$$

we can deduce

$$\varphi(M) = \begin{cases} \varphi_1 & \text{if } M \in \Omega_1 \\ \frac{1}{2}(\varphi_1 + \varphi_2) & \text{if } M \in S \\ \varphi_2 & \text{if } M \in \Omega_2 \end{cases} = \int_S -(\varphi_1 - \varphi_2)|_S \mathbf{n}(M') \cdot \nabla' G(M, M')\, dS'\,. \tag{4.28}$$

Thus, for two-phase flow systems without solid boundaries, the potential in each phase is generated by the dipole distribution

$$\tau = \varphi_1|_S - \varphi_2|_S\,. \tag{4.29}$$

If we examine the velocity fields, they may be of course written under an integral representation by differentiation of Eqs. (4.28)

$$\mathbf{v}(M) = \begin{cases} \mathbf{v}_{(1)} & \text{if } M \in \Omega_1 \\ \frac{1}{2}(\mathbf{v}_{(1)} + \mathbf{v}_{(2)}) & \text{if } M \in S \\ \mathbf{v}_{(2)} & \text{if } M \in \Omega_2 \end{cases} = \nabla \int_S \tau(M')\mathbf{n}(M') \cdot \nabla G(M, M')\, dS'\,. \tag{4.30}$$

We shall give now an integral representation of $\mathbf{v}$ in terms of a vortex distribution, but to do so, a first transformation of Eqs. (4.30) is necessary. By use of classical identities we have

$$\mathbf{v}(M) = \nabla \times \int_S -\tau(M')\mathbf{n}(M') \times \nabla G(M, M')\, dS'\,. \tag{4.31}$$

Under this form, we can see that the velocity field $\mathbf{v}$ are derived from the vector potential

$$\mathbf{A}(M) = \int_S -\tau(M')\mathbf{n}(M') \times \nabla G(M, M')\, dS'\,. \tag{4.32}$$

Now,

$$\nabla_S[\tau(M')G] = \tau(M')\nabla_S G + G\nabla_S \tau\,, \tag{4.33}$$

where the symbol ∇_S denotes the surface gradient with the differentiation taken with respect to M'. Then the vector potential can be written in the form

$$\mathbf{A}(M) = \int_S \mathbf{n}(M') \times \nabla_S(\tau G)\, dS' - \int_S G(\mathbf{n}(M') \times \nabla_S \tau)\, dS'\,. \tag{4.34}$$

Strictly speaking, this transformation is only valid for Case 1 where, by means of the Stokes formula, the first integral is shown to be zero. In Case 2, the same result is obtained but through a slightly different line of reasoning. The starting point is not given by Eqs. (4.30) but by a similar equation involving distributions over $\Sigma(t)$ and over $\partial\mathcal{R}$. We are then led to an equation equivalent to Eq. (4.34) with S replaced by Σ in the two integrals, and extra contributions from the surface of the sphere $\partial\mathcal{R}$. The Stokes formula gives

$$\int_{\partial\Sigma} \tau\, dl' \times \nabla' G \tag{4.35}$$

for the first integral; it vanishes as $1/R^3$ at the same time as the extra contribution from $\partial\mathcal{R}$ when $R \to \infty$, since from (3.11) $\tau = O(1/R^2)$. Thus

$$\mathbf{v}(M) = \int_S [-\mathbf{n}(M') \times \nabla_S \tau] \times (\nabla' G)\, dS' . \tag{4.36}$$

Comparing this formula with the classical Biot–Savart law, it appears that the field $\mathbf{v}$ is generated by a vortex-sheet over S, the intensity of which is

$$\gamma = -\mathbf{n} \times \nabla_S \tau . \tag{4.37}$$

Finally from (4.36) we could return to the scalar potential in order to express it in terms of γ instead of τ as in (4.41) (see SEDOV [45]) but here the expression (4.36) is sufficient as we shall see later on.

We have seen in this chapter that velocity fields $\mathbf{v}_{(k)}$ and potential fields φ_k, $k = 1, 2$ can be expressed in terms of either a distribution of dipoles τ over S, or a distribution of vortices γ. Different systems of equations governing these densities are given in the next section.

5. Boundary integral methods for fluid-fluid systems

5.1. Preliminaries

In the previous section, we have seen integral formulation for the potential fields φ_k, $k = 1, 2$, and for the velocity fields $\mathbf{v}_{(k)}$, $k = 1, 2$. These formulations, expressed in terms of dipoles or vortices, are valid at all times, and we must now specify how they evolve over time. The global system of equations that we have at our disposal is composed of two parts. The first part describes kinematics of the two fluid flows and is precisely given by the integral equation (4.30) or (4.36) which replaces equations (3.8), (3.11) and (3.13) at once. The second part deals with dynamics and includes equation (3.14) and the initial conditions (3.16) at the surface. It includes also the Bernoulli equations (3.9) but not in Ω_k, $k = 1, 2$; the limiting form of these equations at the dividing surface S is sufficient

$$\left.\frac{\partial \varphi_k}{\partial t}\right|_S = -\left[\frac{1}{2}\mathbf{v}_{(k)}^2 + \psi_k + \frac{1}{\varrho_k} p_k\right]\Bigg|_S , \quad k = 1, 2 . \tag{5.1}$$

The above form is not convenient for calculations on a surface. In Sect. 2 we have seen that in that application two surface markers may be envisaged, the classical "Lagrangian markers" or fictitious particles attached to a non-drifting coordinate system. To express time variations of surface fields, here the field τ, it has also been shown in this section that there are two frames of reference: the neighbouring space system of coordinates $\{x_i;\ i = 1, 2, 3\}$ fixed in $\mathcal{E}$ and a non-drifting surface system of coordinates $\{\tilde{y}^\alpha;\ \alpha = 1, 2\}$. The first system of reference is only possible when the field, as in our case, is also defined in the neighbouring 3-D region. In our calculations we shall need both systems of reference. It is basically more simple to use the second type of markers although the first one is of some interest. Indeed, when dealing with the surface system of coordinates, it is easily seen that

$$\tilde{y}^\alpha = y_f^\alpha , \quad \alpha = 1, 2 \tag{5.2}$$

and

$$\left.\frac{\partial \tilde{y}^\alpha}{\partial t}\right|_{y_f^\Gamma} = 0 = \mathbf{w}_{ft} \cdot \tilde{\mathbf{a}}^\alpha = w_{ft}^\alpha, \quad \alpha = 1,2. \tag{5.3}$$

Several simplifications will result from Eqs. (5.3). With this type of marker, the fictitious material derivative of $\varphi_k|_S$ is written, taking into account Eq. (2.23)

$$\frac{d_s}{dt}\varphi_k|_S = \frac{\partial \varphi_k|_S}{\partial t} + \nabla\varphi_k|_S \cdot w_n = \frac{\partial \varphi_k|_S}{\partial t} + w_n \nabla\varphi_k|_S \cdot n = \frac{\partial \varphi_k|_S}{\partial t} + w_n^2. \tag{5.4}$$

Thus Eq. (5.1) becomes

$$\frac{d_s}{dt}\varphi_k|_S = w_n^2 - \left[\frac{1}{2}\mathbf{v}_{(k)}^2 + \psi_k + \frac{1}{\varrho_k}p_k\right]\Big|_S. \tag{5.5}$$

We shall now present two different methods for solving the above set of equations. The first one proceeds from the "generalized vortex method" introduced by BMO [4] for 2-D calculations. The second method, proposed by ROBERTS [43], will appear as a generalization of the so-called "Bernoulli's methods" commonly used to solve free-boundary value problems.

Referring to the equivalence between dipole and vortex distributions presented in the previous section, each method can also be treated in terms of γ distributions. In the following, the two methods (and their two γ-variants) are described in detail and are compared with each other.

5.2. The "generalized vortex method"

An equation for $d_s\tau/dt$ is easily obtained by subtracting the two equations (5.5)

$$\begin{aligned}\frac{d_s}{dt}(\varphi_2 - \varphi_1)|_S &= -\frac{d_s}{dt}\tau \\ &= -\frac{1}{2}(\mathbf{v}_{(2)}^2 - \mathbf{v}_{(1)}^2)|_S - (\psi_2 - \psi_1)|_S - \left(\frac{1}{\varrho_2}p_2 - \frac{1}{\varrho_1}p_1\right)\Big|_S,\end{aligned} \tag{5.6}$$

and by using Eqs. (3.14) and (3.15)

$$-\frac{d_s}{dt}\tau = -\frac{1}{2}(\mathbf{v}_{(2)}^2 - \mathbf{v}_{(1)}^2)|_S + \Psi - \left(\frac{1}{\varrho_2} - \frac{1}{\varrho_1}\right)p_1|_S + \frac{1}{\varrho_2}2HT. \tag{5.7}$$

Now adding the two equations (5.5) gives

$$\frac{d_s}{dt}(\varphi_2 + \varphi_1)|_S = 2w_n^2 - \frac{1}{2}(\mathbf{v}_{(1)}^2 + \mathbf{v}_{(2)}^2)|_S - (\psi_1 + \psi_2)|_S - \left(\frac{1}{\varrho_1}p_1 + \frac{1}{\varrho_2}p_2\right)\Big|_S. \tag{5.8}$$

We have on the surface, from Eq. (4.28),

$$\varphi(M) = \frac{1}{2}(\varphi_1 + \varphi_2) = \int_{S(t)} -\tau(M',t)\mathbf{n}(M') \cdot \nabla' G(M,M')\, dS', \tag{5.9}$$

where we have re-introduced the time dependence, so Eq. (5.8) becomes

$$2\frac{d_s}{dt}\varphi = 2w_n^2 - \frac{1}{2}(\mathbf{v}_{(1)}^2 + \mathbf{v}_{(2)}^2)|_S - (\psi_1 + \psi_2)|_S - \left(\frac{1}{\varrho_1} + \frac{1}{\varrho_2}\right)p_1|_S + \frac{1}{\varrho_2}2HT. \tag{5.10}$$

The final equation for $d_s\tau/dt$ is obtained by eliminating the pressure terms between Eqs. (5.7) and (5.10), and by using the integral form (5.9) for φ:

$$(5.11)\quad (\varrho_1+\varrho_2)\frac{d_s}{dt}\tau = 2(\varrho_1-\varrho_2)\frac{d_s}{dt}\left\{\int_{S(t)} -\tau(M',t)\mathbf{n}(M')\cdot\nabla' G(M,M')\,dS'\right\}$$
$$-2(\varrho_1-\varrho_2)w_n^2+\varrho_1\mathbf{v}_{(1)}^2-\varrho_2\mathbf{v}_{(2)}^2+(\varrho_1+\varrho_2)\Psi+(\varrho_1-\varrho_2)(\psi_1+\psi_2)-4HT\,.$$

Now we want to calculate the time derivative of the integral in the RHS with the help of Appendix 2. This expression is first considered on $\Sigma(t)$ which is an arbitrary subsurface of $S(t)$ bounded by a line $\partial\Sigma(t)$ consisting of the chosen markers (5.2)

$$(5.12)\quad \frac{d_s}{dt}\int_{\Sigma(t)}\tau(M',t)K(M,M')\,dS'$$
$$=\frac{d_s}{dt}\int\int_{y_f[\Sigma(t)]}\tau[M'(y_f^1,y_f^2,t),t]K[M,M'(y_f^1,y_f^2,t)]\sqrt{a_f}\,dy_f^1\,dy_f^2\,,$$

where

$$(5.13)\quad K(M,M') = -\mathbf{n}(M')\cdot\nabla' G(M,M')\,.$$

The resulting form which can be compared to (A.2.6), is the starting point of derivation leading to the surface transport theorem. This theorem gives finally in our case

$$(5.14)\quad \frac{d_s}{dt}\int_{\Sigma(t)}\tau K\,dS' = \int_{\Sigma(t)}\left(\frac{d_s\tau}{dt}K+\frac{d_sK}{dt}\tau+K\tau\,\mathrm{div}_s\,\mathbf{w}_f\right)dS'\,.$$

Here, all fictitious material time derivatives are taken by using a surface system of coordinates $\{\tilde{y}^\alpha;\ \alpha=1,2\}$, contrary to Eq. (5.5) where the space system $\{x_i;\ i=1,2,3\}$ has been used. In the integral in the RHS of Eq. (5.14), the two last terms have to be made clear. First we have

$$\frac{d_sK}{dt} = -\frac{d_s\mathbf{n}}{dt}\cdot\nabla' G-\mathbf{n}\cdot\frac{d_s\nabla' G}{dt}\,.$$

The first time derivative is given by Eqs. (2.28) and (2.29), and the second one can be written in the form

$$\frac{d_s\nabla' G}{dt} = \left[\frac{\partial^2 G}{\partial x'^i\partial x'^j}\mathbf{g}^i+\frac{\partial G\partial\mathbf{g}^k}{\partial x'^k\partial x'^j}\right]\frac{dx'^j}{dt}\bigg|_{y_f^\Gamma} = \left[\frac{\partial^2 G}{\partial x'^i\partial x'^j}-\frac{\partial G}{\partial x'^k}\Gamma_{ij}^k\right]\mathbf{g}^i(\mathbf{w}_f\cdot g^j)$$
$$=\left[3\left(\frac{\frac{\partial s}{\partial x'^i}\frac{\partial s}{\partial x'^j}}{s^5}\right)-\frac{\delta^{ij}}{s^3}+\Gamma_{ij}^k\left(\frac{\frac{\partial s}{\partial x'^k}}{s^3}\right)\right](\mathbf{g}^i\otimes\mathbf{g}^j)\mathbf{w}_f\,.$$

Secondly, we obviously have

$$\mathrm{div}_s\,\mathbf{w}_{ft} = 0\,,$$

or with (A.2.16)

$$(5.15)\quad \mathrm{div}_s\,\mathbf{w}_f = -2Hw_n\,,$$

which shows simplifications resulting from the use of non-drifting markers. Finally, letting $\Sigma(t) \to S(t)$ in Cases 1 and 2, we obtain a new expression which is inserted in Eq. (5.11)

$$(5.16)\quad (\varrho_1 + \varrho_2)\frac{d_s}{dt}\tau = 2(\varrho_1 - \varrho_2)\int_{S(t)} \left[\frac{d_s\tau}{dt}K + \tau\left(\frac{d_sK}{dt} - 2HKw_n\right)\right] dS'$$
$$-2(\varrho_1 - \varrho_2)w_n^2 + \varrho_1\mathbf{v}_{(1)}^2 - \varrho_2\mathbf{v}_{(2)}^2 + (\varrho_1 + \varrho_2)\Psi + (\varrho_1 - \varrho_2)(\psi_1 + \psi_2) - 4HT.$$

If we consider τ and the velocity fields $\mathbf{v}_{(k)}$ as given, Eq. (5.16) appears as a Fredholm integral equation of the second kind for $d_s\tau/dt$, which can be used in order to update values of τ at the next time step. (Refer to Table 1 for the general flowchart of this method.)

Consider now the same problem expressed in γ-distribution. Referring to the previous section, γ is such that

$$(5.17)\quad \gamma = -\mathbf{n} \times \nabla_s\tau.$$

The starting point of the calculations still is Eq. (5.11) on which the operator $-\mathbf{n} \times \nabla_S$ is applied. Equation (5.11) is thus transformed into

$$(5.18)\quad -(\varrho_1 + \varrho_2)\frac{d_s}{dt}\gamma = -\mathbf{n} \times \left\{2(\varrho_1 - \varrho_2)\frac{d_s}{dt}\left[\frac{1}{2}(\mathbf{v}_{(1)} + \mathbf{v}_{(2)})\right] - 2(\varrho_1 - \varrho_2)\nabla_s w_n^2\right.$$
$$\left. + \varrho_1\nabla\mathbf{v}_{(1)}^2 - \varrho_2\nabla\mathbf{v}_{(2)}^2 + 2(\varrho_1 - \varrho_2)\mathbf{F} + 4T\nabla_s H\right\} \quad \text{on } S.$$

Furthermore

$$(5.19)\quad \frac{1}{2}(\mathbf{v}_{(1)} + \mathbf{v}_{(2)}) = \int_S \gamma(M') \times \nabla' G(M, M')\, dS'.$$

Hence,

$$(5.20)\quad -(\varrho_1 + \varrho_2)\frac{d_s}{dt}\gamma = -\mathbf{n} \times \left\{2(\varrho_1 - \varrho_2)\frac{d_s}{dt}\int_S \gamma(M') \times \nabla' G(M, M')\, dS'\right.$$
$$\left. -2(\varrho_1 - \varrho_2)\nabla_s w_n^2 + \varrho_1\nabla\mathbf{v}_{(1)}^2 - \varrho_2\nabla\mathbf{v}_{(2)}^2 + 2(\varrho_1 - \varrho_2)\mathbf{F} + 4T\nabla_s H\right\}.$$

The time derivative of the integral in the RHS of the last equation would be expressed in a similar way to that for the dipole distribution, and we should obtain a Fredholm integral equation of the second kind for $d_s\gamma/dt$ instead of $d_s\tau/dt$.

We are now able to replace the "generalized vortex method" of BMO [4] among other methods using vortex sheets. According to Eq. (5.17) it can be seen, as is well known in the potential theory, that a vortex sheet generates a discontinuity for the velocity values

$$(5.21)\quad [\mathbf{v}_{(2)} - \mathbf{v}_{(1)}]|_S \times \mathbf{n} = \gamma.$$

For this reason, vortex sheets have been extensively used for modelling sharp variations of tangential velocities in a thin layer dividing a mass of otherwise irrotational fluid. In simple cases where problems are two-dimensional, this description leads to the classical "point vortex method" (used since Rosenhead, 1931) where each point vortex retains a

constant vorticity and is convected under the flow induced by the others. In fully three-dimensional flows, a similar "line vortex method" could be envisaged and, in this case, the vorticity of each line would vary with the stretching of the line, as indicated by the Helmholtz theorem. In our problem of two-phase motion, the two last terms in Eq. (5.20) show that the density jump and the gradient of curvature are at the origin of the initial vorticity. In this connection, as underlined by BMO [3], this is similar to the baroclinic creation of vorticity in a non-homogeneous fluid, a creation specified by the Bjerknes theorem (YIH [52]). It must be emphasized that the forms of Eq. (5.16) or (5.20) are simpler for two-dimensional problems. This is the reason why it has been used in this particular case by BMO [4], and several other authors (TELSTE [49], KERR [23]).

5.3. The "generalized Bernoulli method"

Calculations now are based again on the same system. First we combine the two equations (5.5) in order to eliminate the pressure terms

$$\frac{d_s}{dt}\Phi = (\varrho_2 - \varrho_1)w_n^2 - \frac{1}{2}(\varrho_2 \mathbf{v}_{(2)}^2 - \varrho_1 \mathbf{v}_{(1)}^2)|_S - \varrho_2\psi_2|_S + \varrho_1\psi_1|_S - 2HT\,. \tag{5.22}$$

This equation introduces the time derivative of a new surface potential

$$\Phi = \varrho_2\varphi_2|_S - \varrho_1\varphi_1|_S\,. \tag{5.23}$$

Table 1. Comparison of the two classes of Boundary Integral Methods for fluid-fluid systems, in the dipole representation. a) Generalized vortex method (BAKER, MEIRON and ORSZAG [4]). b) Generalized Bernoulli's method (alternative method used in this paper, first presented by ROBERTS [43]).

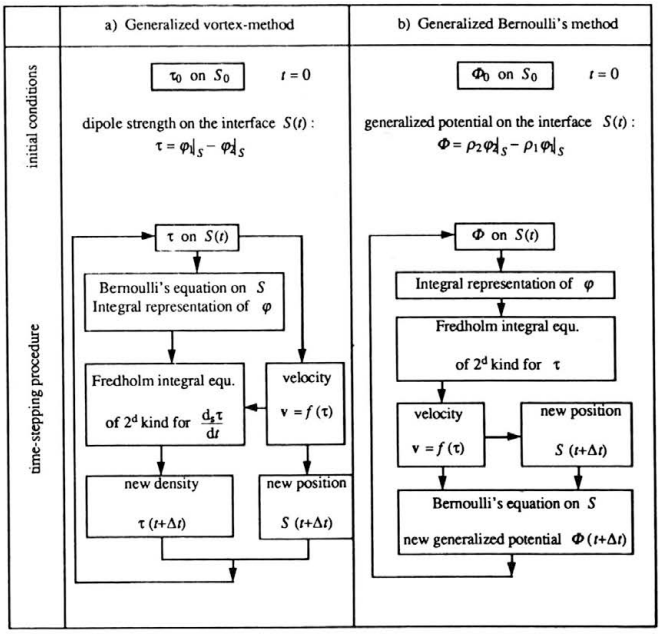

Decomposing this quantity by use of Eq. (4.19) gives

$$\Phi = -\left(\frac{\varrho_1 + \varrho_2}{2}\right)\tau + (\varrho_2 - \varrho_1)\varphi|_S \,, \tag{5.24}$$

and using Eq. (5.9)

$$\Phi = -\left(\frac{\varrho_1 + \varrho_2}{2}\right)\tau + (\varrho_2 - \varrho_1) \int_{S(t)} -\tau(M')\mathbf{n}(M') \cdot \nabla' G(M, M')\, dS' \,. \tag{5.25}$$

If we consider Φ as a given function, Eq. (5.25) is a Fredholm integral equation of the second kind for the unknown density τ. Then, velocity fields can be computed and Eq. (5.25) allows us to update at the next time step. This method generalizes the one employed in cavitation or free-surface problems. When one deals with a single phase flow with a free-surface condition, over which the pressure is kept constant, the resolution of Laplace's equation for the scalar potential, coupled with given potential values on the boundaries (Dirichlet problem) furnishes the velocity field, and then Bernoulli's equation can be used for updating the potential on the free-surface S. This procedure, first employed by PLESSET, CHAPMAN [38] in the frame of finite differences computation, has been re-employed later on (BMO [4], BLAKE *et al.* [9] and recently by LUNDGREN, MANSOUR [29] using integral representations over the free-surface. Thus, our method appears to be a generalization of these "Bernoulli methods", since it can easily handle the two-phase motion by introducing the generalized potential (5.23). For a comparison with the previous method, Table 1 presents the flowcharts of the two methods in their dipole representation. Let us now look at the variant method employing the γ-distribution. In a way similar to the first method, if we apply the operator $-\mathbf{n} \times \nabla_s$ to Eq. (5.24), we obtain

$$\varrho_2(\mathbf{v}_{(2)} \times \mathbf{n}) - \varrho_1(\mathbf{v}_{(1)} \times \mathbf{n}) = \left(\frac{\varrho_1 + \varrho_2}{2}\right)\gamma - (\varrho_2 - \varrho_1)\mathbf{n} \times \left[\frac{1}{2}(\mathbf{v}_{(1)} + \mathbf{v}_{(2)})\right] . \tag{5.26}$$

Let's denote

$$\mathbf{V} = -\mathbf{n} \times \nabla_s \Phi = \varrho_2(\mathbf{v}_{(2)} \times \mathbf{n}) - \varrho_1(\mathbf{v}_{(1)} \times \mathbf{n}) \tag{5.27}$$

which is a weighted average of the tangential velocities above and below the interface. So, by virtue of Eq. (5.19), we have finally

$$\mathbf{V} = \left(\frac{\varrho_1 + \varrho_2}{2}\right)\gamma - (\varrho_2 - \varrho_1)\mathbf{n} \times \int_S \gamma(M') \times \nabla' G(M, M')\, dS' \,, \tag{5.28}$$

and the transformation of Eq. (5.22) by the same operator furnishes

$$\frac{d_s}{dt}\mathbf{V} = -\left\{(\varrho_2 - \varrho_1)\nabla_s w_n^2 - \frac{1}{2}(\varrho_2 \nabla \mathbf{v}_{(2)}^2 - \varrho_1 \nabla \mathbf{v}_{(1)}^2)|_S - (\varrho_2 - \varrho_1)\mathbf{F} + 2T\nabla_s H\right\} . \tag{5.29}$$

Hence, if we consider $\mathbf{V}$ as a given surface function, Eq. (5.29) is a Fredholm equation of the second kind for the density γ. Then the velocity fields can be derived and Eq. (5.29) is used to update γ at the next time step.

Let us come back now to the comparison of the two methods a) and b). Examine the time derivative of the integral term in Eqs. (5.11) or (5.20). One can easily see that the new method presented in b) is more direct than the classical one of BMO 82, except however for 2-D problems, for which the latter authors performed the calculations in the complex plane.

Table 2. Overview of boundary integral formulations for irrotational fluid-fluid motions.

First class : Vortex methods	Second class : Bernoulli's methods	
surface of discontinuity in one fluid $\frac{\rho_1}{\rho_2} = 1$ Kelvin's theorem $\rightarrow$ $\frac{d_s\gamma}{dt} = 0$ γ : vortex strength on S Rosenhead, 1931 (P.V.M) Fink & Soh, 1978 (P.V.M) Baker, 1980 (P.V.M) P.V.M. = Point-Vortex Method	free-surface flow $\frac{\rho_1}{\rho_2} = 0$ (one fluid + one passive medium) Bernoulli's equation $\rightarrow$ $\frac{d_s\varphi}{dt}$ on S φ : velocity potential Plesset & Chapman, 1971 (finite differences) Lenoir, 1976 (variational method) Blake & Gibson, 1981 (B.I.M.; sources) Baker et al., 1984 (B.I.M.; dipoles) Blake et al., 1986 (B.I.M.; sources + dipoles) B.I.M. = Boundary Integral Method	mother-methods
Fredholm integral equation for $\frac{d_s\tau}{dt}$ (Baker, Meiron & Orszag, 1982)	Fredholm integral equation for τ via $\Phi = \rho_2\varphi_2\big\|_S - \rho_1\varphi_1\big\|_S$ Bernoulli's equ. $\rightarrow$ $\frac{d_s\Phi}{dt}$ (Roberts, 1983)	dipole distribution : $\tau = \varphi_1\big\|_S - \varphi_2\big\|_S$ velocity fields induced by : Generalized methods for fluid-fluid systems
Fredholm integral equation for $\frac{d_s\gamma}{dt}$ (Baker, Meiron & Orszag, 1982)	Fredholm integral equation for γ via $\mathbf{V} = \rho_2(\mathbf{n}\times\mathbf{v}_{(2)}\big\|_S) - \rho_1(\mathbf{n}\times\mathbf{v}_{(1)}\big\|_S)$ Bernoulli's equ. $\rightarrow$ $\frac{d_s\mathbf{V}}{dt}$	vortex distribution : $\gamma = -\mathbf{n}\times(\mathbf{v}_{(2)}\big\|_S - \mathbf{v}_{(1)}\big\|_S)$

All the above described methods are included in Table 2, which includes the "mother-methods".

6. Application to axisymmetric flows

6.1. Small vibrations of a spherical globule

In this first application, the generalized Bernoulli method is used to describe small oscillations of a fluid globule (bubble or drop) of a spherical form; this globule is surrounded by another fluid which extends to infinity. If the oscillations of the surface of the globule are very small compared to its radius, then it is well known (LAMB [25]) that any axisymmetric oscillation may be written as a sum of spherical harmonics S_n, which are solutions, or modes, of the linearized problem. So we have, in spherical coordinates:

$$r(\theta) = a\left(1 + \sum_{n\geq 1} \varepsilon_n S_n\right), \tag{6.1}$$

where a is the mean radius of the globule, ε_n the amplitude of the n-th mode, such that

$$\varepsilon_n \ll 1. \tag{6.2}$$

The spherical harmonics have the form

$$S_n = P_n(\cos\theta)\cos(\omega_n t + \beta_n), \tag{6.3}$$

where P_n is the Legendre polynomial of order n, ω_n the pulsation of this mode and β_n

its phase. In the context of linear oscillations, we have

$$\omega_n^2 = \frac{n(n+1)(n-1)(n+2)}{[(n+1)\varrho_1 + n\varrho_2]} \cdot \frac{T}{a^3}, \tag{6.4}$$

where T is the surface tension and ϱ_1, ϱ_2 are, respectively, density of the internal and external fluids. As we are only interested in the oscillations of the globule surface and not in its translation, we may eliminate the gravity, so that the potential energy per unit mass of each fluid introduced in Sect. 3 is zero,

$$\psi_1 = \psi_2 = 0. \tag{6.5}$$

We limit these test-calculations to the numerical study of the second mode, the initial conditions are fixed, so that

$$\beta_2 = 0 \tag{6.6}$$

whereas the two fluid are at rest

$$\varphi_{k,0} = 0 \quad \text{in} \quad \Omega_k, \quad k = 1,2 \quad \text{at} \quad t = 0. \tag{6.7}$$

No assumptions are made about the values of the density ϱ_1 and ϱ_2. We are going now to apply the method developed in Sect. 5.3, in its dipole representation, so that the set of required equations corresponds to Eqs. (5.22), (5.23) and (5.25); these equations are written in a dimensionless form:

$$\frac{d_s}{dt}\Phi^* = -2Aw^{*2} + \frac{1}{2}(1+A)\mathbf{v}_{(1)}^{*2} - \frac{1}{2}(1-A)\mathbf{v}_{(2)}^{*2} + 2H^*, \tag{6.8}$$

$$\Phi^* = (1-A)\varphi_2^* - (1+A)\varphi_1^*, \tag{6.9}$$

$$\Phi^* = -\tau^* + 2A \int_{S(t)} -\tau^* \mathbf{n}(M') \cdot \nabla'^* G^*(M, M')\, dS'^*. \tag{6.10}$$

The dimensionless form obtained results from the choice of the mean radius a for the characteristic length and T/a for the characteristic pressure difference. The initial conditions become

$$r^*(\theta) = 1 + \xi^* = 1 + \varepsilon_2 S_2 \quad \text{at} \quad t^* = 0 \tag{6.11}$$

and

$$\Phi_0^* = 0 \quad \text{at} \quad t^* = 0. \tag{6.12}$$

The only non-dimensional parameter which appears in Eqs. (6.8)–(6.10) is the Atwood ratio

$$A = \frac{\varrho_1 - \varrho_2}{\varrho_1 + \varrho_2}. \tag{6.13}$$

Note that the surface tension T, which is the only forcing term, does not appear explicitly in Eq. (6.13) but is contained in the time scale.

The numerical discretization of the set (6.8), (6.10) is derived in Appendix 3. The Fortran code of our model has been implemented on a mini-computer Apollo (DN 3000 station) and takes about 5 mn of CPU time for a run of 500 time steps.

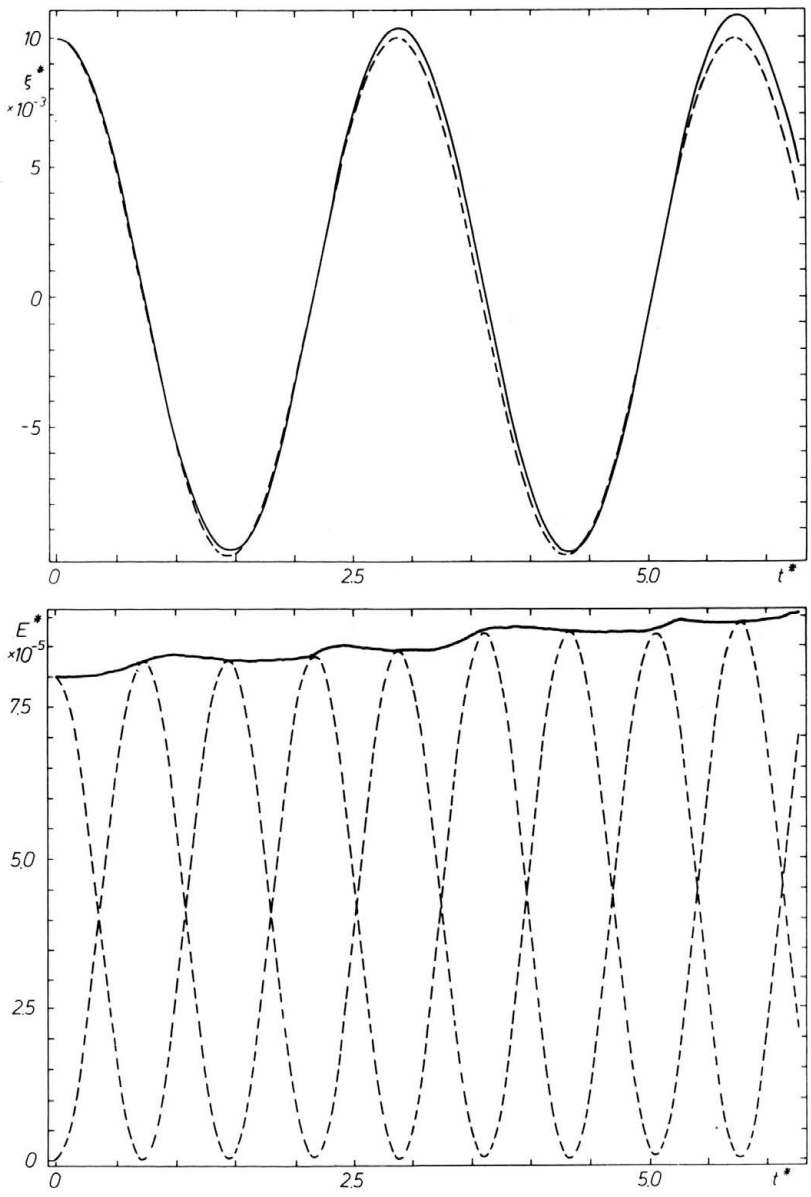

FIG. 5. Linear oscillations of a spherical globule: $A = 0$, $N = 20$ points, $f = 0.05$.
a) perturbation ξ^* at the top of the globule (continuous line).
The dashed line is the theoretical curve.
b) kinetic and potential energy (dashed lines); their sum is represented by the continuous line.

phenomena as well as industrial processes. In all cases, this instability increases the interface area and leads to greater mixing due to the penetration of one fluid in the other. Linear studies have been made for a long time by TAYLOR [48] for the 2-D case and by CHANDRASEKHAR [13] for axially symmetric and 3-D cases. The nonlinear behaviours have been computed by BMO [3] using the vortex method, and by PROSPERRETI, JACOBS

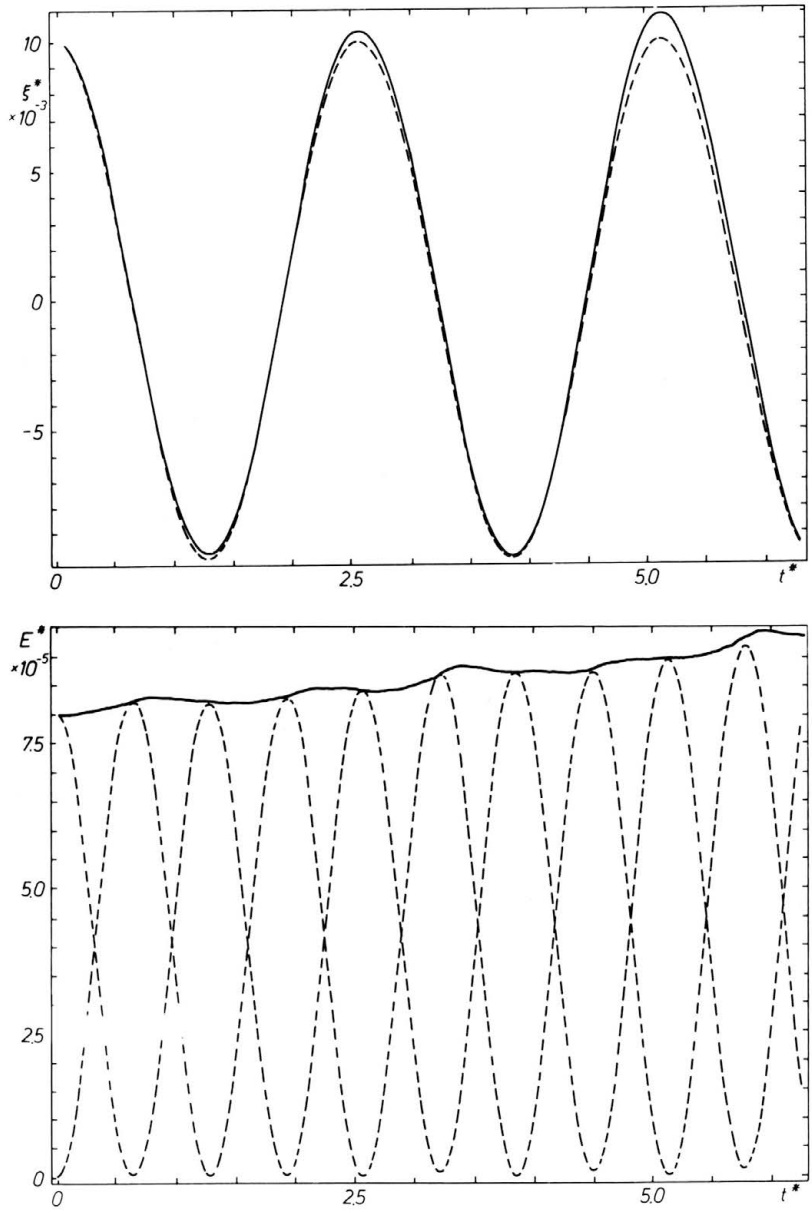

FIG. 4. Linear oscillations of a spherical globule: $A = -1$, $N = 20$ points, $f = 0.05$.
a) perturbation ξ^* at the top of the globule (continuous line).
The dashed line is the theoretical curve.
b) kinetic and potential energy (dashed lines); their sum is represented by the continuous line.

6.2. Axisymmetric Rayleigh-Taylor instability

The second application deals with a classical problem, namely the Rayleigh–Taylor instability in an unbounded fluid-fluid system. This problem has been the subject of both experimental and theoretical studies, some typical applications being related to natural

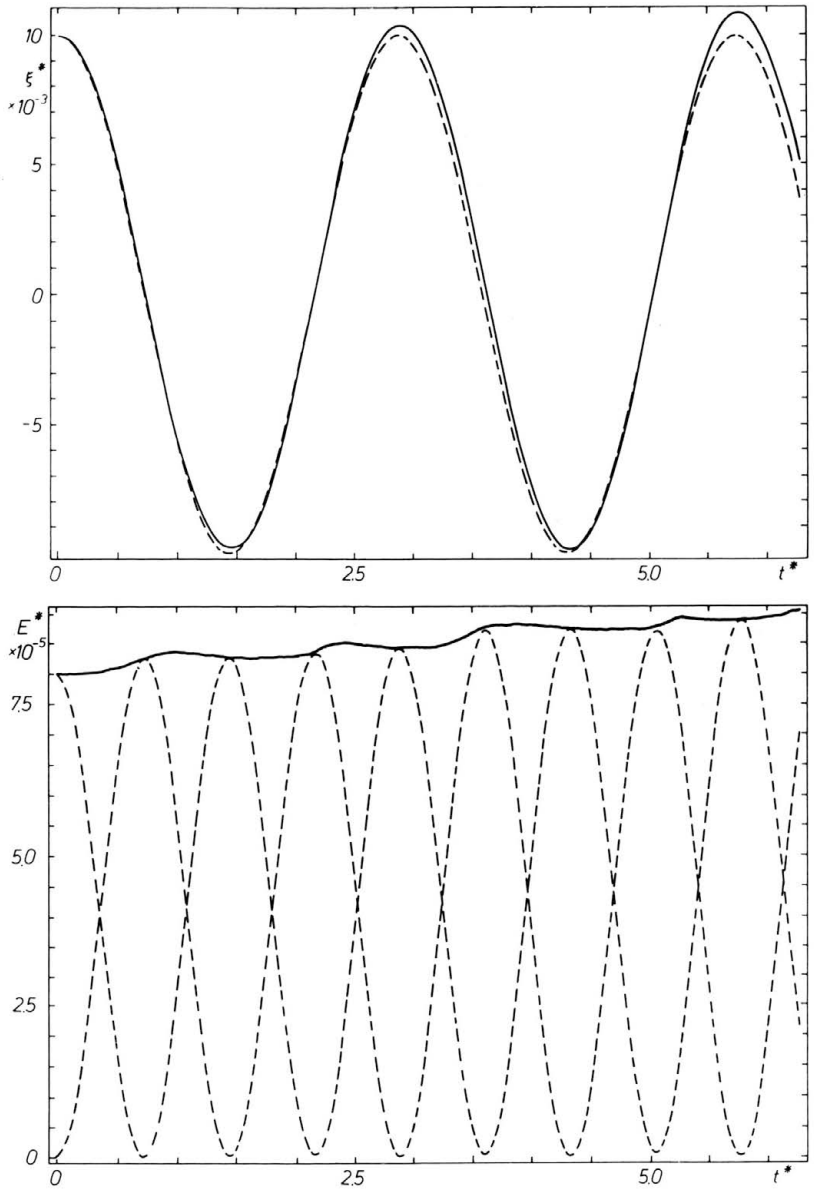

FIG. 5. Linear oscillations of a spherical globule: $A = 0$, $N = 20$ points, $f = 0.05$.
a) perturbation ξ^* at the top of the globule (continuous line).
The dashed line is the theoretical curve.
b) kinetic and potential energy (dashed lines); their sum is represented by the continuous line.

phenomena as well as industrial processes. In all cases, this instability increases the interface area and leads to greater mixing due to the penetration of one fluid in the other. Linear studies have been made for a long time by TAYLOR [48] for the 2-D case and by CHANDRASEKHAR [13] for axially symmetric and 3-D cases. The nonlinear behaviours have been computed by BMO [3] using the vortex method, and by PROSPERRETI, JACOBS

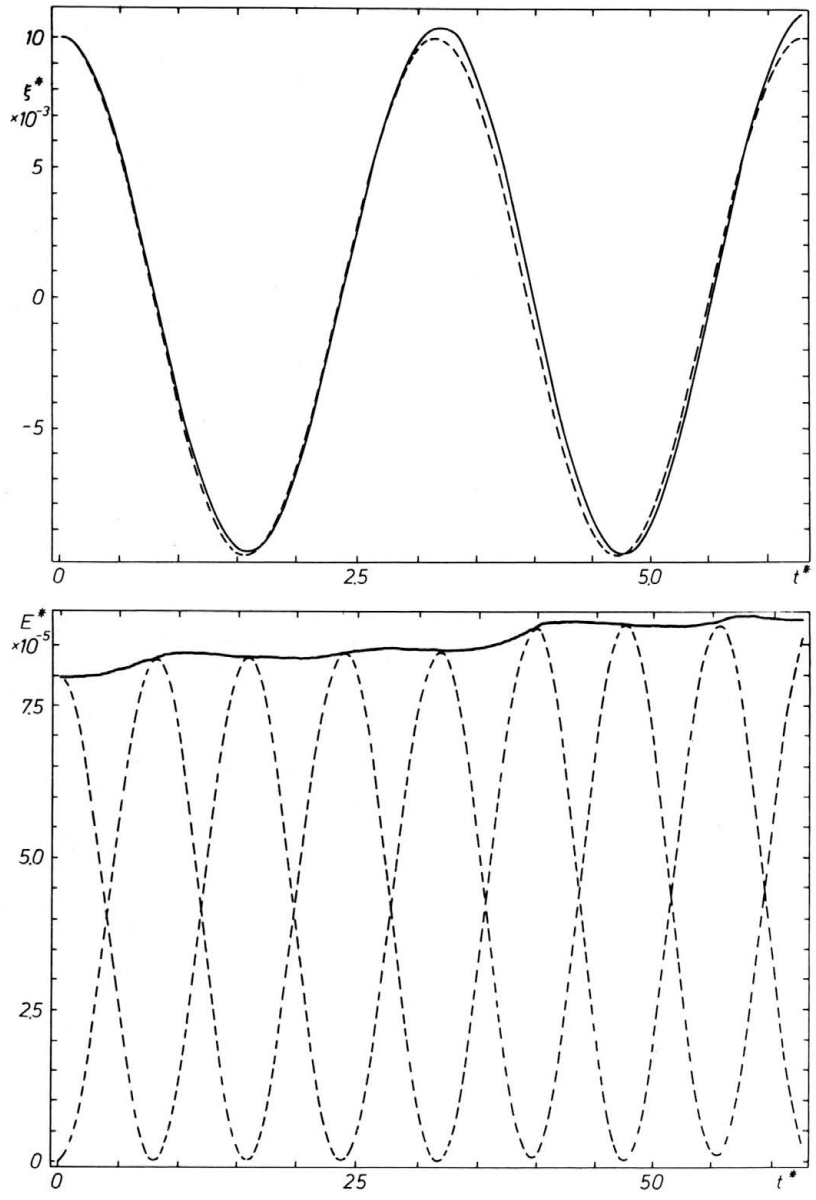

FIG. 6. Linear oscillations of a spherical globule: $A = +1$, $N = 20$ points, $f = 0.05$.
a) perturbation ξ^* at the top of the globule (continuous line).
The dashed line is the theoretical curve.
b) Kinetic and potential energy (dashed lines); their sum is represented by the continuous line.

[40] using a finite difference method, for 2-D irrotational motions. Other methods have been applied to the same phenomenon taking into account the full Navier-Stokes equations (DALY [14], ZUFIRIA [53]).

The two fluids introduced at the beginning of this paper may have either the same density, or different ones. They are initially separated by a plane interface which extends

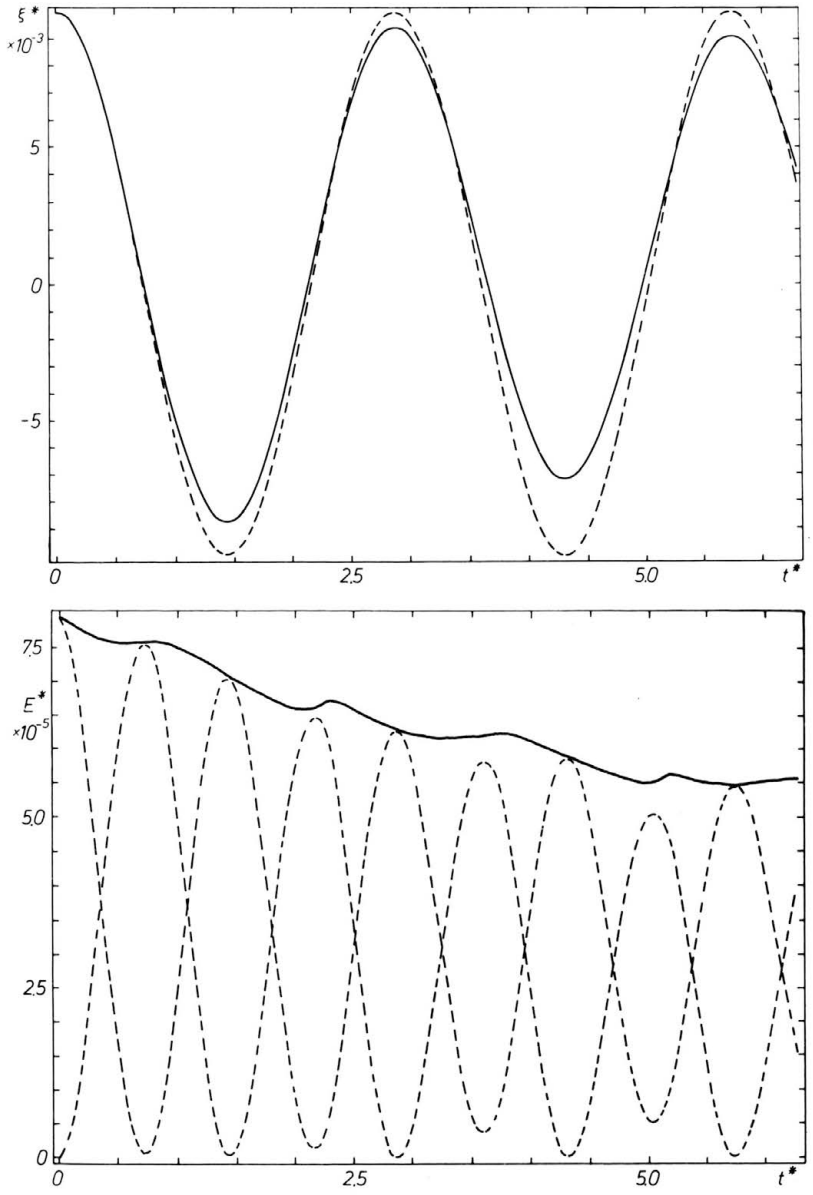

FIG. 7. Linear oscillations of a spherical globule—influence of the smoothing factor: $A = 0$, $N = 20$ points, $f = 0.20$. a) perturbation ξ^* at the top of the globule (continuous line). The dashed line is the theoretical curve, b) kinetic and potential energy (dashed lines); their sum is represented by the continuous line.

to infinity, so Eq. (3.14) takes the particular asymptotic form

$$\left.\begin{aligned} H &\to 0 \\ (p_1 - p_2)|_S &\to 0 \end{aligned}\right\} \quad \text{as} \quad r \to \infty . \tag{6.16, 6.17}$$

Gravity acts downwards along the z-axis (see Fig. 8) and its intensity is denoted by g.

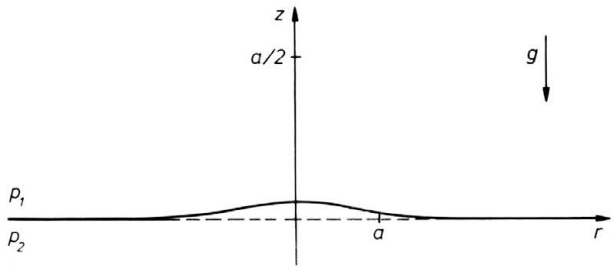

FIG. 8. Initial conditions for the axisymmetric Rayleigh–Taylor problem. The dashed line represents the equilibrium position of the interface. The perturbation shape is of Gaussian form (note that the scale in the z-direction has been magnified). This configuration corresponds to the Case 2 defined in Sect. 2.

We impose the equilibrium position of the interface to be the plane $z = 0$.

Because of axial symmetry, all variables depend only on the cylindrical coordinates (r, z), $r \geq 0$. The pressure value on the interface at infinity is denoted by p_∞, so the potentials ψ_k of the body forces introduced in Sect. 3 are

$$\psi_1 = gz - \frac{1}{\varrho_1} p_\infty , \tag{6.17}$$

$$\psi_2 = gz - \frac{1}{\varrho_2} p_\infty \tag{6.18}$$

according to Eq. (3.12).

Initially, the perturbation shape is chosen to be of Gaussian form

$$z_s = b_0 \exp\left(-\frac{r^2}{a^2}\right) \quad \text{at} \quad t = 0 , \tag{6.19}$$

where a is an arbitrary length, the two fluids are at rest

$$\varphi_{k,0} = 0 \quad \text{in} \quad \Omega_k , \quad k = 1, 2 \quad \text{at} \quad t = 0 \tag{6.20}$$

and the denser fluid lies above the less dense one

$$\varrho_1 \geq \varrho_2 \geq 0 \tag{6.21}$$

so that, under the action of the forces of gravity, the configuration is unstable.

We are going now to apply our method in its dipole representation, so the set of the equations required corresponds to Eqs. (5.22), (5.23) and (5.25). In order to recast the above set of equation into a dimensionless form, we refer all distances to a characteristic length of the initial shape of S, say a which is the radius in Eq. (6.17), and the velocity fields $\mathbf{v}_{(k)}$, $k = 1, 2$ — to the characteristic velocity U_0. The time scale is equal to a/U_0. The pressure difference fields $p_k - p_\infty$, $k = 1, 2$ are made dimensionless by introducing a characteristic pressure difference field Δp. Assuming that the inertia and pressure terms are always of the same order of magnitude in problems where the irrotational hypothesis is of some interest, the last two scales will be chosen such that

$$\Delta p = \frac{1}{2}(\varrho_1 + \varrho_2) U_0^2 .$$

In some cases, the scale U_0 is given and Δp deduced. In other cases the converse is true, as e.g. in cavitation problems where Δp is the pressure difference between that at infinity and the saturated vapour inside the bubble.

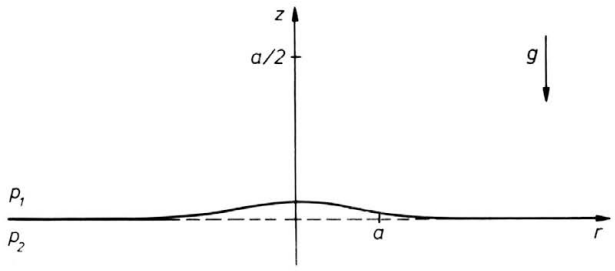

FIG. 8. Initial conditions for the axisymmetric Rayleigh–Taylor problem. The dashed line represents the equilibrium position of the interface. The perturbation shape is of Gaussian form (note that the scale in the z-direction has been magnified). This configuration corresponds to the Case 2 defined in Sect. 2.

We impose the equilibrium position of the interface to be the plane $z = 0$.

Because of axial symmetry, all variables depend only on the cylindrical coordinates (r, z), $r \geq 0$. The pressure value on the interface at infinity is denoted by p_∞, so the potentials ψ_k of the body forces introduced in Sect. 3 are

$$\psi_1 = gz - \frac{1}{\varrho_1} p_\infty , \tag{6.17}$$

$$\psi_2 = gz - \frac{1}{\varrho_2} p_\infty \tag{6.18}$$

according to Eq. (3.12).

Initially, the perturbation shape is chosen to be of Gaussian form

$$z_s = b_0 \exp\left(-\frac{r^2}{a^2}\right) \quad \text{at} \quad t = 0 , \tag{6.19}$$

where a is an arbitrary length, the two fluids are at rest

$$\varphi_{k,0} = 0 \quad \text{in} \quad \Omega_k , \quad k = 1, 2 \quad \text{at} \quad t = 0 \tag{6.20}$$

and the denser fluid lies above the less dense one

$$\varrho_1 \geq \varrho_2 \geq 0 \tag{6.21}$$

so that, under the action of the forces of gravity, the configuration is unstable.

We are going now to apply our method in its dipole representation, so the set of the equations required corresponds to Eqs. (5.22), (5.23) and (5.25). In order to recast the above set of equation into a dimensionless form, we refer all distances to a characteristic length of the initial shape of S, say a which is the radius in Eq. (6.17), and the velocity fields $\mathbf{v}_{(k)}$, $k = 1, 2$ — to the characteristic velocity U_0. The time scale is equal to a/U_0. The pressure difference fields $p_k - p_\infty$, $k = 1, 2$ are made dimensionless by introducing a characteristic pressure difference field Δp. Assuming that the inertia and pressure terms are always of the same order of magnitude in problems where the irrotational hypothesis is of some interest, the last two scales will be chosen such that

$$\Delta p = \frac{1}{2}(\varrho_1 + \varrho_2) U_0^2 .$$

In some cases, the scale U_0 is given and Δp deduced. In other cases the converse is true, as e.g. in cavitation problems where Δp is the pressure difference between that at infinity and the saturated vapour inside the bubble.

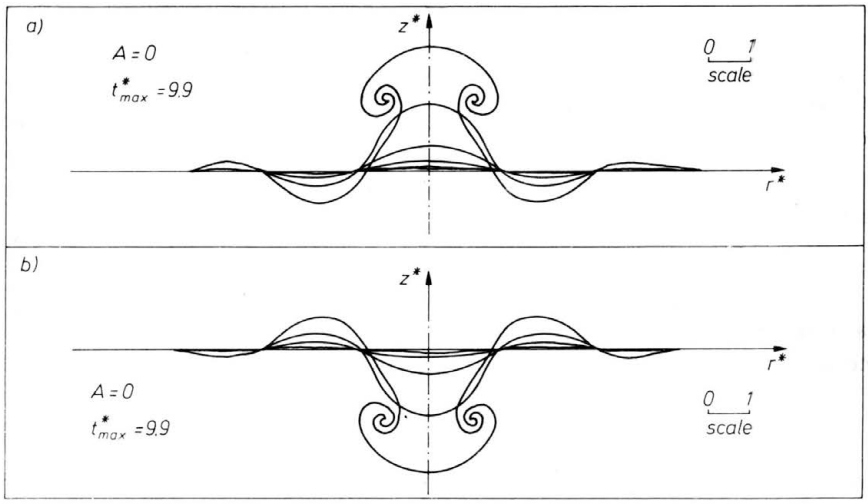

FIG. 9. Influence of the Atwood ratio A for the axisymmetric Rayleigh–Taylor instability for Eotvos number $E = 6.0$. Each figure represents the upward (a) and downward (b) growth. The shape of the interface has been plotted at evenly spaced points from $t^* = 0$ to $t^* = t^*_{max}$. The values of t^*_{max} and A are shown in each figure.

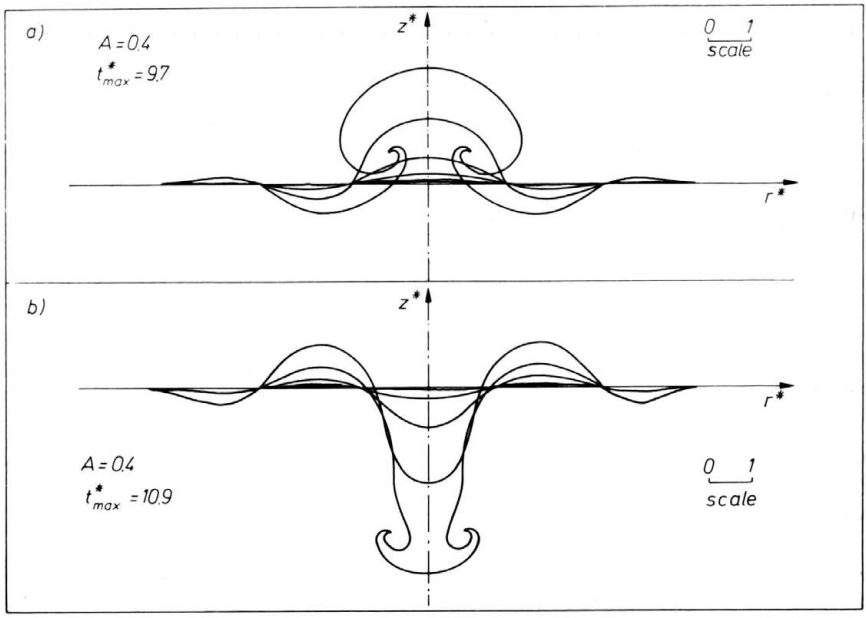

FIG. 10. Influence of the Atwood ratio A for the axisymmetric Rayleigh–Taylor instability for Eotvos number $E = 6.0$. Each figure represents the upward (a) and downward (b) growth. The shape of the interface has been plotted at evenly spaced points from $t^* = 0$ to $t^* = t*_{max}$. The values of t^*_{max} and A are shown in each figure.

However, our system is always unstable, since the initial Gaussian shape contains all the "wavelength" λ.

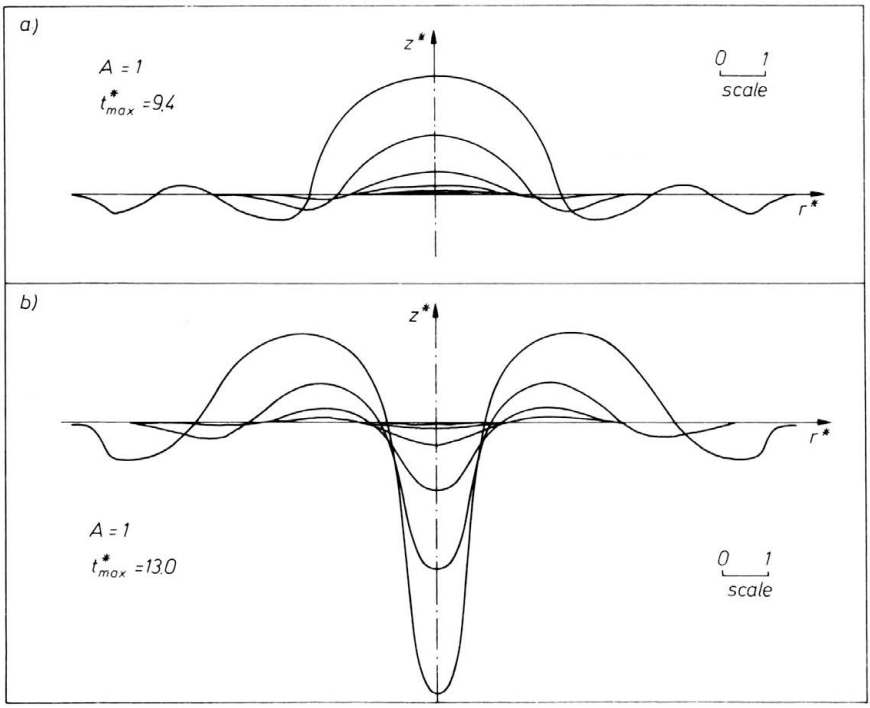

FIG. 11. Influence of the Atwood ratio A for the axisymmetric Rayleigh–Taylor instability for Eotvos number $E = 6.0$. Each figure represents the upward (a) and downward (b) growth. The shape of the interface has been plotted at evenly spaced points from $t^* = 0$ to $t^* = t^*_{max}$. The values of t^*_{max} and A are shown in each figure.

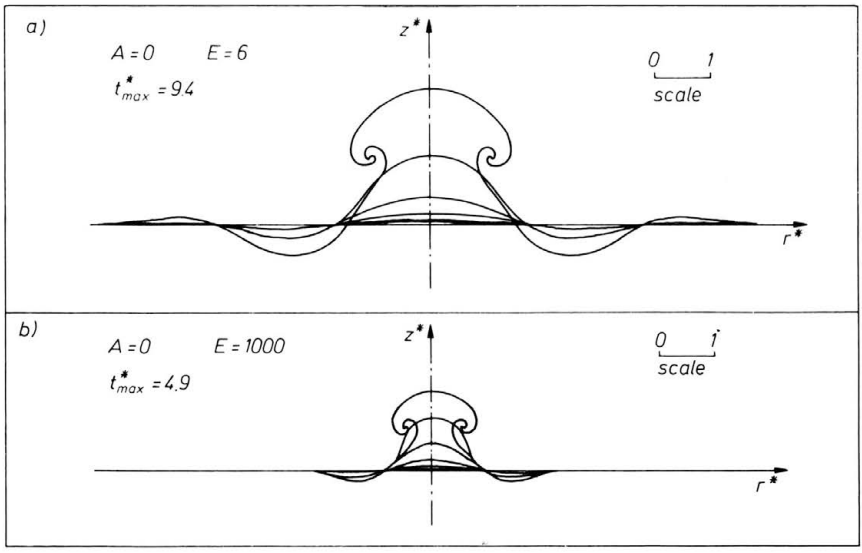

FIG. 12. Influence of the Eotvos number E (see also the caption of Figs. 9 to 11).

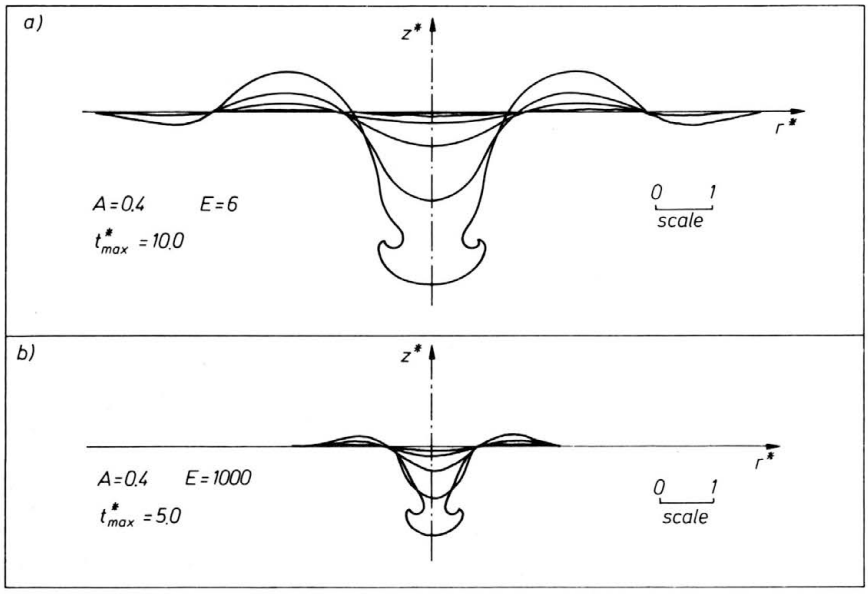

FIG. 13. Influence of the Eotvos number E (see also the caption of Figs. 9 to 11).

Secondly, the Atwood ratio A characterizes the difference of density between the two fluids. Since we impose $\varrho_1 \geq \varrho_2$, the range of A which can be covered is $[0, 1]$. Two limiting cases then arise and are especially interesting.

The first one is $A = 0$. If we keep the Eotvos number not equal to zero, by supposing that gravity g tends to infinity as the product $(\varrho_1 - \varrho_2)g$ remains constant, we then have the case of two immiscible fluids of the same density in presence of surface tension: this is the Boussinesq approximation. With an infinite Eotvos number (no surface tension), we have simply a surface of discontinuity in the same fluid occupying the two domains Ω_1 and Ω_2.

The second one is $A = 1$, which corresponds to one dense fluid above a passive medium: this is the classical approximation made for gas-liquid systems, corresponding to the condition (3.17).

In all the cases presented now, the initial surface is represented by $N = 30$ points, distributed from the axis $r^* = 0$ to $r^* = 15$, with a height $b_0^* = \pm 0.05$. The initial time-step is 0.05, and the lower limit allowed in our code is 10^{-5}. A typical run of 140 time steps uses 15 mm of CPU time, with a number of nodes rising from 30 up to 120.

Upward and downward growths of the Gaussian perturbation for $A = 0, 0.4, 1$ have been plotted in Figs. 9 to 11. These simulations show well known features according to the Atwood ratio. In the case $A = 0$ (Fig. 9; two fluids of the same density) we observe a mushroom-like formation, with a perfect symmetry between the growth up and down to gravity, whereas in the case $A = 1$ (Fig. 11; liquid above vacuum), a bubble formation or a spike-jet pattern is observed according to the direction of the initial perturbation. The last dissymmetric behaviours are consistent with the experimental investigations of LEWIS [27]. The influence of the Eotvos number mainly changes the scale of the phenomenon (see Figs. 9 and 12) together with its time scale. In all

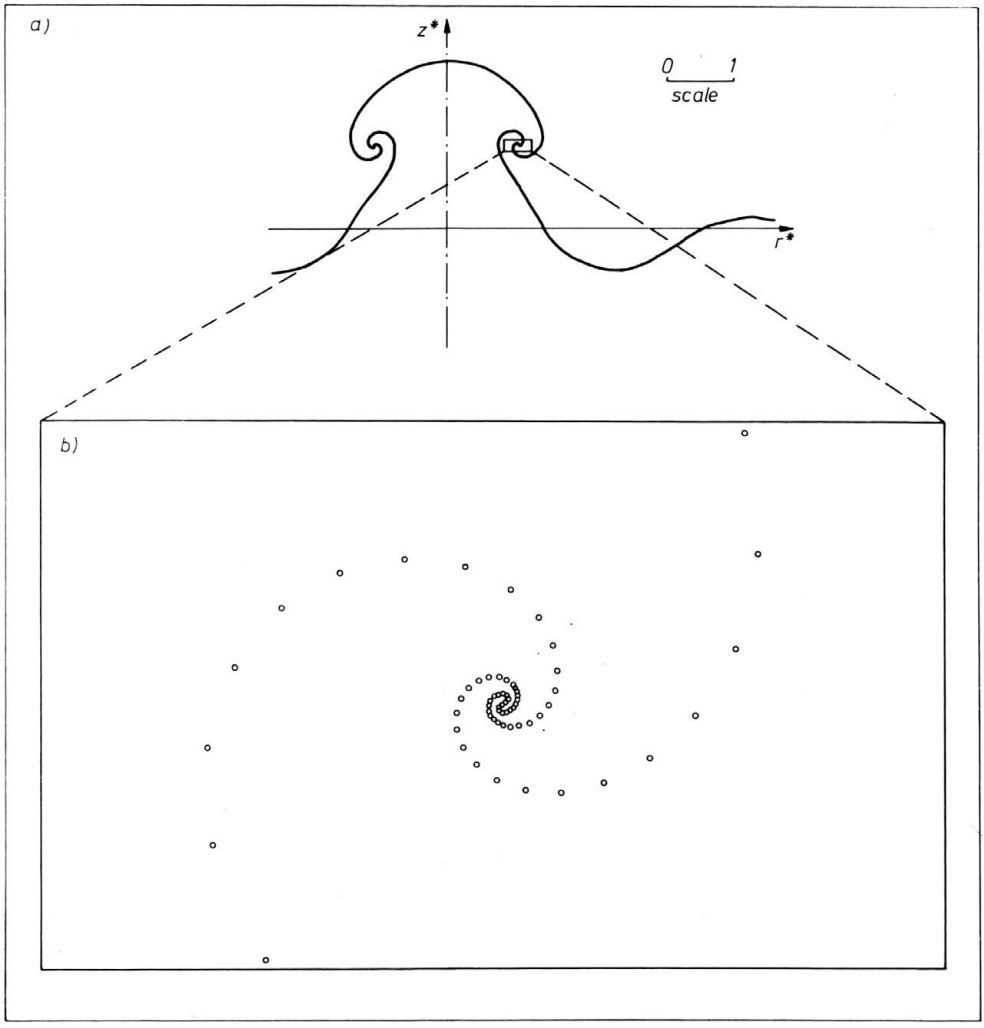

FIG. 14. Formation of a shape singularity on the interface at a finite time. $A = 0$, $E = 6$; a) shape of the interface at $t^*_{max} = 9.4$; b) enlarged view of the "roll-up".

the cases studied (Figs. 9 and 12) the time evolution was stopped by strong singularities in the shape of the surface, so that the number of points rapidly reached 200, the upper limit arbitrarily fixed in our code. These singularities which arise at a finite time, taking the form of a roll-up (see Fig. 14) when the Atwood ratio is close to zero, corresponding to the development of a Kelvin-Helmholtz instability, or taking the form of a cusp (see Fig. 15) otherwise, have been described in the literature concerning the evolved vortex-sheets (PULLIN [41], MEIRON et al. [31], KRASNY [24], RANGEL, SIRIGNANO [42]). From the study of the latter paper, the introduction of the surface tension in the range of instability does not always eliminate the singularity. The same result appears in the work of PULLIN [41] and in the present simulations.

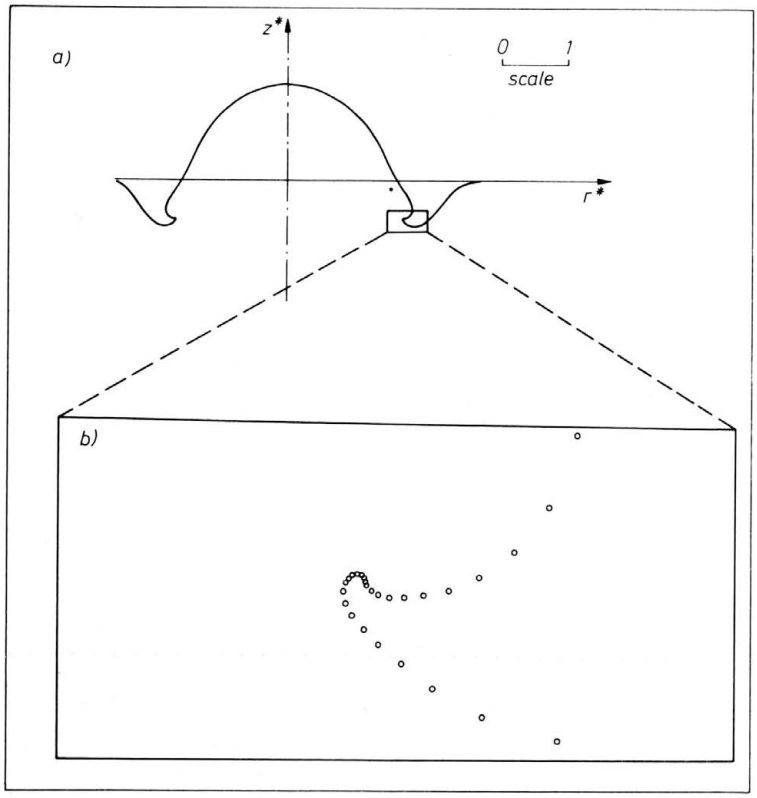

FIG. 15. Formation of a shape singularity on the interface at a finite time. $A = 0.8$, $E = 6$; a) shape of the interface at $t^*_{max} = 9.0$; b) enlarged view of the "cusp".

We might think that the viscous effects eliminate these singularities, and smooth the roll-up formation, but it is worth noticing that simulations of the Navier-Stokes equations for the same phenomenon by a marker-and-cell method also exhibit a strong roll-up for small Atwood ratios (DALY [14]).

In the present simulations, a smoothing procedure is employed whose principal effect is to delay the appearance of the singularity (see Fig. 16). In other respect, the smoothing is equivalent to a fictitious dissipation at the interface, and it seems dangerous to use strong smoothing because there is no longer a physical description of the phenomenon. Recently, many efforts have been made to eliminate these singularities. TRYGGVASON [51] used a modified vortex-in-cell method; KERR [23] applied the vortex-blob technique to the BMO [4] method, together with a modification of the meshing during the time evolution. These two authors worked only on 2-D problems. Similar regularizing procedure, just as high-order schemes described in Appendix 3, should be applied to the present method. However, the application treated here clearly shows that interesting results can be obtained as a result of a very simple approach, and also demonstrates its simplicity and flexibility.

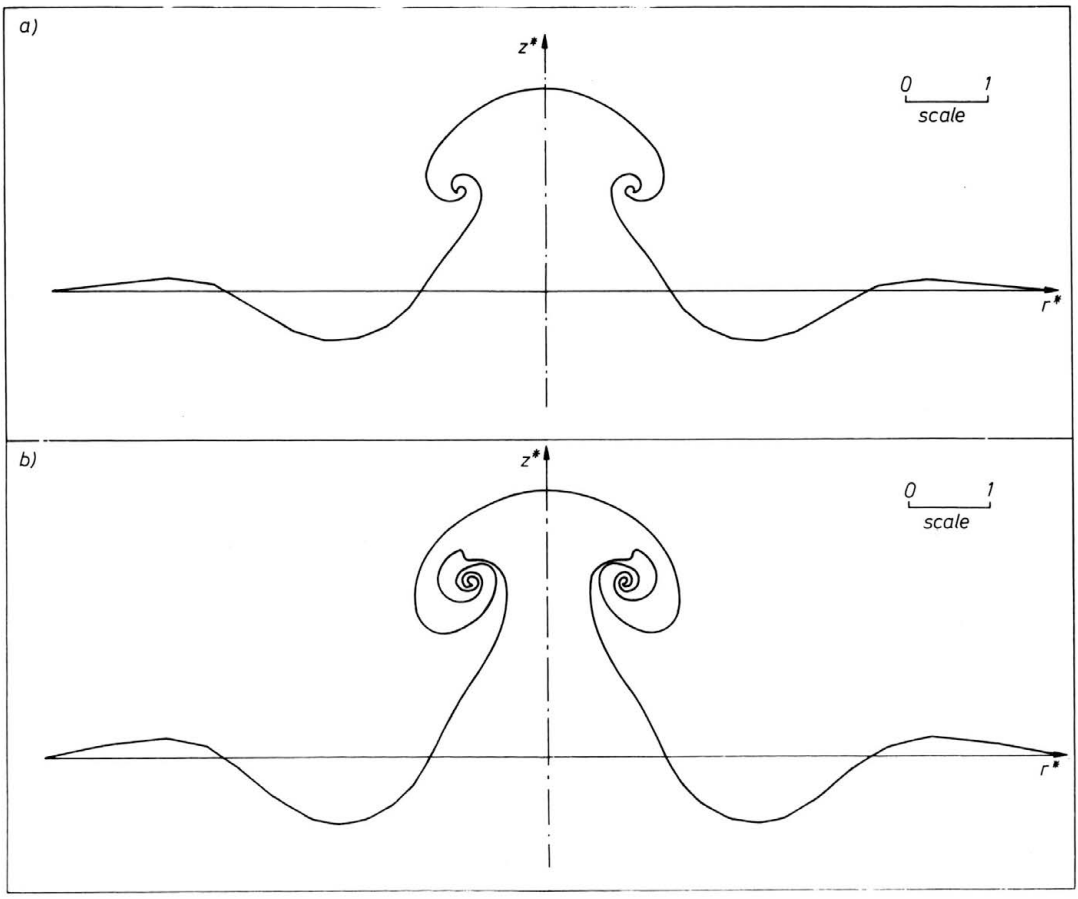

FIG. 16. Smoothing effects on the time evolution of the interface. $A = 0$, $E = 6$.
In case b) the smoothing factor is one fourth of that in case a); a) $t^*_{max} = 9.4$, b) $t^*_{max} = 10.2$.

7. Conclusion

In this paper, an overview of possible boundary integral formulations for irrotational incompressible fluid-fluid system has been given in a systematical way. It has been shown that two classes of methods are available; the first one, known as the "generalized vortex method" was established by BAKER, MEIRON, ORSZAG [4] and is an extension of the classical "point-vortex method". We have shown that it may be expressed using either a dipole or a vortex representation and, moreover, that it can have a three-dimensional version. The second one, due to ROBERTS [43], appears to be an extension of some "Bernoulli methods", and it has also two possible representations. Table 2 presents all these methods and their relations. The aim of this article was not to compare the numerical efficiency or stability of the two methods mentioned above. However, as shown in Sect. 5, the Bernoulli method can be derived in a more straightforward way than the other one, especially in the three-dimensional case.

Several extensions or further applications may be envisaged. For simplicity, we have limited ourselves to configurations such as those shown in Figs. 1 or 2. However, the

various methods can be used when several inclusions of different fluids are dispersed in another fluid. Fluids can also be bounded by solid boundaries, fixed or moving (BAKER et al. [4], TELSTE [49]) under the condition that solid boundaries and interfaces do not intersect each other. Moving contact lines deserve a special study which is in progress.

Another possible extension is the presence of compressible inclusions (without inertia) and characterized by a uniform and varying pressure field. To express the volume variations in such a case, a point-source may be located within each inclusion; this situation is reminiscent of the work of BLAKE and GIBSON [8], where a source distribution close to the interior surface of their cavitation has been introduced.

Appendix 1. Meshing of a smooth line

Although it may be extended to define proper distribution of panels on a surface, this method will be restricted to generate a distribution of boundary elements on a plane curve, i.e. series of straight-line segments. Actually the final application is only axisymmetric and basic ideas of this method will not be obscured by the complex formalism of the surface representation. For a curve, equations corresponding to Eq. (2.3) are

$$x^i = x_c^i(u), \quad i = 1,2 \tag{A.1.1}$$

or, in a vectorial form

$$\mathbf{x} = \mathbf{x}_c(u). \tag{A.1.2}$$

The time t has been omitted. The curve coordinate u, which is assumed to be positively oriented, is then given at any time as resulting from the transport of the previous parametrization, and it is supposed to require some adjustments. In order to make calculations easier, a preliminary transformation must be done from u to s, the arc-length parameter of the curve and then, what is specifically looked for, is a local increasing transformation

$$\bar{u} = \bar{u}(s) \tag{A.1.3}$$

which meets two requirements: local smoothness and adaptation of the segments to the variations of a function F. First, recall some obvious approximate mathematical representations of the segments and of variation of those segments. In the new unknown approximation, consider a segment whose initial point is $\mathbf{x}_c(\bar{u})$ and endpoint is $\mathbf{x}_c(\bar{u}+\Delta\bar{u})$, $\Delta\bar{u}$ being an arbitrary difference, constant for any segment. The vector

$$\Delta\mathbf{x}_c(\bar{u}) = \mathbf{x}_c(\bar{u} + \Delta\bar{u}) - \mathbf{x}_c(\bar{u}) \tag{A.1.4}$$

representing the segment, is given by

$$\Delta\mathbf{x}_c(\bar{u}) = \frac{ds}{du}\Delta\bar{u}\mathbf{t} + o(\Delta\bar{u}), \tag{A.1.5}$$

where $\mathbf{t} = d\mathbf{x}_c/ds$ is the unit tangent vector. Another approximation, concerning the difference between two successive segments, is given by

$$\Delta\mathbf{x}_c(\bar{u} + \Delta\bar{u}) - \Delta\mathbf{x}_c(\bar{u}) = \left[\frac{d^2s}{d\bar{u}^2}\mathbf{t} + \left(\frac{ds}{d\bar{u}}\right)^2 \kappa\mathbf{n}\right](\Delta\bar{u})^2 + o(\Delta\bar{u})^2, \tag{A.1.6}$$

where κ is the normal curvature and $\mathbf{n}$ is the unit normal. A mesh will be considered as locally smooth if two subsequent segments have:

1) two orientations differing by less than the given amount $\theta_{\max}$

$$\theta \cong (\Delta\overline{u})^2 \left(\frac{ds}{d\overline{u}}\right)^2 \kappa \Big/ \left(\frac{ds}{d\overline{u}}\Delta\overline{u}\right) \leq \theta_{\max}; \tag{A.1.7}$$

2) two component magnitudes along $\mathbf{t}$ differing by less than the given amount $r_{\max}$

$$(\Delta\overline{u})^2 \left|\frac{d^2 s}{d\overline{u}^2}\right| \Big/ \left(\frac{ds}{d\overline{u}}\Delta\overline{u}\right) \leq r_{\max}. \tag{A.1.8}$$

The last constraint is introduced only for numerical precision purposes, as shown in the classical "point-vortex method" by FINK, SOH [18]. Further, the mesh will be considered as adapted to the space evolution of a given strictly positive weight function F, if:

3) the product of F by the segment length is smaller than a constant

$$\frac{ds}{d\overline{u}}\Delta\overline{u}F(s) \leq c. \tag{A.1.9}$$

The function F reflects the fact that the nodes must be concentrated at some place for many reasons: first, to avoid great discrepancies, the segment length must be adapted to the gradient of the function φ which controls the problem (φ is the scalar potential of the velocity field); secondly, some self-crossing of the surface can occur if not enough points are used when different parts of the surface approach one another (BAKER [2], RANGEL, SIRIGNANO [42]).

Our problem, defined by the three above constraints, could be solved by a minimization procedure (a variational approach) which would consist in verifying the constraints globally. Such an approach would be necessary, under some circumstances, in order to have a satisfactory regularity of the mesh during progress in time. This is the true in the case of the Adam's means of several predictor-corrector methods, which compute the next time step by means of several previous time-steps. In this paper, because of the simplicity of our progress in time (see Appendix 3), we don't need such a regularity. We prefer to verify each constraint locally, this procedure furnishing the smallest number of nodes.

Initially, the function

$$g(s) = \frac{ds}{d\overline{u}} = \min\left(\frac{\theta_{\max}}{|\kappa|\Delta\overline{u}}, \frac{c}{F(s)\Delta\overline{u}}\right) \tag{A.1.10}$$

verifies the constraints 1) and 3), and it is possible to correct this function in order to respect the second constraint. Thus, the unknown function $\overline{u}(s)$ is:

$$\overline{u}(s) = \int_0^s \frac{dt}{g(t)}, \tag{A.1.11}$$

which gives also the inverse function $s(\overline{u})$, and the new position of the i-th node is found by the formula

$$s_i = s(i\Delta\overline{u}). \tag{A.1.12}$$

An example of the discretization of the medirian curve of an axisymmetric surface is shown in Fig. 17. It corresponds to an enlarged view of the roll-up of the Fig. 16b. One can see clearly the concentration of nodes (plotted in the form of circles) at places where the curvature is important, or where two portions of the interface come together.

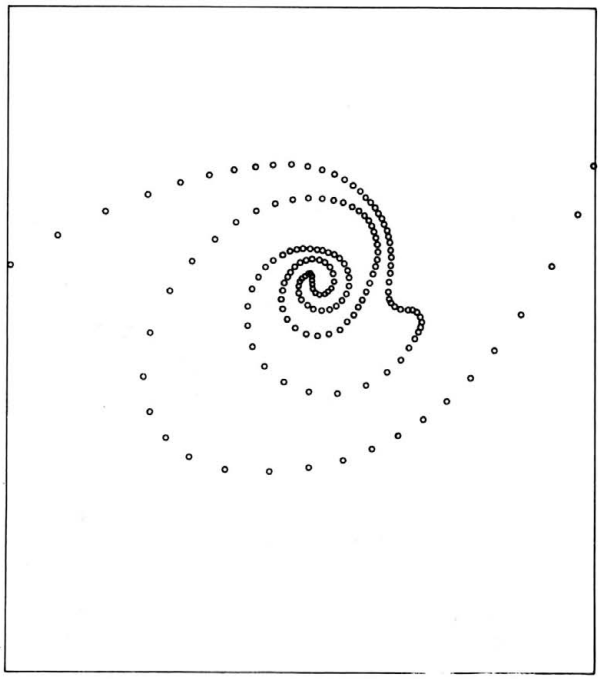

FIG. 17. Example of spatial discretization of the interface by a smooth distribution of nodes.

Appendix 2. Generalized transport surface theorem

Several related theorems appear in the literature (ARIS [1]). We present here a derivation due mainly to DEEMER ad SLATTERY [15].

Let $S(t)$ be a moving surface and $\{\tilde{y}^\alpha;\ \alpha = 1,2\}$ be an arbitrary moving system of non-drifting surface coordinates as defined by Eq. (2.8). A subsurface $\Sigma'(t)$ contained in $S(t)$, bounded by a curve $\partial\Sigma'(t)$, is considered. The curve $\partial\Sigma'(t)$ is assumed to consist all the time of the same material of fictitious particles (say generalized) as defined in Sect. 2. To define $\partial\Sigma'(t)$, a second set of convected coordinates $\{y_f^\Gamma;\ \Gamma = 1,2\}$ is introduced. It can be referred externally to $\{x'^i;\ i = 1,2,3\}$ by Eq. (2.10), or to the first coordinate surface $\{\tilde{y}^\alpha;\ \alpha = 1,2\}$ considered as a surface frame by relation (2.11),

$$\tilde{y}^\alpha = \tilde{y}^\alpha(y_f^1, y_f^2, t), \quad \alpha = 1,2. \tag{A.2.1}$$

Again, this relation can be viewed as giving the location at time t of a generalized particle. The velocity of this particle in space is

$$\left.\frac{\partial x'^i}{\partial t}\right|_{y_f^\Gamma} = w_n n^i_{(1)} + a^i_\alpha \left.\frac{\partial \tilde{y}^\alpha}{\partial t}\right|_{y_f^\Gamma}, \quad i = 1,2,3, \tag{A.2.2}$$

where

$$\left.\frac{\partial \tilde{y}^\alpha}{\partial t}\right|_{y_f^\Gamma} = w_t^\alpha, \quad \alpha = 1,2$$

are the components of the tangential velocity of the generalized particles. Now we want to calculate the rate of change of the following integral extended over the current configuration

$$\frac{d}{dt}\int_{\Sigma'(t)} \psi' \, dS \,, \tag{A.2.3}$$

where ψ' is any scalar or vector-valued function of time and position on $\Sigma'(t)$. Since $\Sigma'(t)$ is covered entirely by $\{\tilde{y}^\alpha;\ \alpha = 1,2\}$, then

$$\int_{\Sigma'(t)} \psi'(M')\, dS' = \int\int_{\tilde{y}[\Sigma'(t)]} \psi' \circ M'(\tilde{y}^1, \tilde{y}^2)\sqrt{\tilde{a}}\, d\tilde{y}^1\, d\tilde{y}^2 \,, \tag{A.2.4}$$

where $\tilde{a}$ is the determinant of the metric tensor relative to $\{\tilde{y}^\alpha;\ \alpha = 1,2\}$ for the surface in the current configuration

$$\tilde{a} = (\det[\tilde{a}_{\alpha\beta}])^{1/2} = (\det[\tilde{\mathbf{a}}_\alpha \cdot \tilde{\mathbf{a}}_\beta])^{1/2} . \tag{A.2.5}$$

The double integral in (A.2.4) is taken over $\tilde{y}[\Sigma'(t)]$ which denotes the set of real numbers $(\tilde{y}^1, \tilde{y}^2)$ corresponding to points in $\mathcal{E}$ belonging to $\Sigma'(t)$. This set is a moving domain in $\mathbf{R}^2$. So, it is not advantageous to differentiate such an integral expression. $\Sigma'(t)$ is also covered by $\{y_f^\Delta;\ \Delta = 1,2\}$, then

$$\int_{\Sigma'(t)} \psi'(M')\, dS' = \int\int_{y_f[\Sigma'(t)]} \psi' \circ M'[\tilde{y}^\alpha(\tilde{y}_f^\Delta, t)]\sqrt{a_f}\, dy_f^1\, dy_f^2 \,, \tag{A.2.6}$$

where a_f is the determinant of the metric tensor relative to $\{y_f^\Delta;\ \Delta = 1,2\}$ for the surface in the current configuration

$$a_f = (\det[a_{f\Delta\Gamma}])^{1/2} . \tag{A.2.7}$$

The double integral in (A.2.6) is particularly convenient for our purposes since it is taken over $y_f[\Sigma'(t)]$ which does not depend on time since its boundary in $\mathbf{R}^2$ consists of pairs of numbers (y_f^1, y_f^2) which are the same at each time. One and two transformations are still necessary. First, under a change of surface coordinates from convected to non-drifting ones, $\sqrt{a_f}$ obeys the transformation rule

$$\sqrt{a_f} = \sqrt{\tilde{a}}J \,, \tag{A.2.8}$$

where

$$J = \det\left[\frac{\partial \tilde{y}^\alpha}{\partial y_f^\Delta}\right]$$

is the Jacobian of the transformation (A.2.1). Note that such a change would allow to recover the double integral in (A.2.4) from the double integral in (A.2.6). Working on with the convected coordinates, we will use, nevertheless, (A.2.8) in (A.2.6) because then the resulting integrand

$$\psi'\sqrt{\tilde{a}}J \,,$$

where

$$\psi'[y_f^\Delta, t] = \psi' \circ M'[\tilde{y}^\alpha(y_f^\Delta, t)]$$

can be more easily differentiated with respect to time. This is the starting point of many derivations for the surface transport theorem (ARIS [1]).

Secondly, it may be interesting to introduce the determinant of the metric tensor relative to $\{y_f^\Delta;\ \Delta = 1,2\}$ for the surface in the reference configuration

$$a_r = (\det[a_{r\Delta\Gamma}])^{1/2}. \tag{A.2.9}$$

The RHS of (A.2.6) becomes

$$\int\int_{y_f[\Sigma'(t)]} \psi' \sqrt{a} J \, dy_f^1 \, dy_f^2 = \int\int_{y_f[\Sigma_r']} \psi' \frac{\sqrt{a}}{\sqrt{a_r}} J \sqrt{a_r} \, dy_f^1 \, dy_f^2 , \tag{A.2.10}$$

where the following identity has been used

$$y_f[\Sigma'(t)] = y_f[\Sigma_r'] \quad \text{for all} \quad t . \tag{A.2.11}$$

Then we can write

$$\int\int_{y_f[\Sigma_r']} \psi' \frac{\sqrt{\tilde{a}}}{\sqrt{a_r}} J \sqrt{a_r} \, dy_f^1 \, dy_f^2 = \int_{\Sigma_r'} \psi' D' \, dS_r , \tag{A.2.12}$$

where

$$D' = \frac{\sqrt{\tilde{a}}}{\sqrt{a_r}} J$$

denotes the surface expansion. These terms can be easily explained by comparing the RHS of (A.2.12) and the LHS of (A.2.6),

$$D' = \frac{dS}{dS_r} . \tag{A.2.13}$$

Consider an element of material surface at (y_f^1, y_f^2) defined by the increments dy_f^Δ of each coordinate in the reference configuration; its area is dS_r. Due to the motion, this element is moved and distorted, so its new area is $D' \, dS_r$.

Now we are in position to evaluate (A.2.3). We find by using (A.2.12).

$$\begin{aligned} \frac{d}{dt} \int_{\Sigma'(t)} \psi' \, dS &= \frac{d}{dt} \int_{\Sigma_r'} \psi' D' \, dS_r \\ &= \int_{\Sigma_r'} \left(\psi' \frac{d_s D'}{dt} + D' \frac{d_s \psi'}{dt} \right) dS_r = \int_{\Sigma'(t)} \left(\psi' \frac{1}{D'} \frac{d_s D'}{dt} + \frac{d_s \psi'}{dt} \right) dS , \end{aligned} \tag{A.2.14}$$

where the last RHS has been obtained by returning to the current configuration. Use is made of the following basic result

$$\frac{1}{D'} \frac{d_s D'}{dt} = \operatorname{div}_s \mathbf{w}_t - 2H w_n , \tag{A.2.15}$$

the RHS of which can be transformed according to the classical identity

$$\operatorname{div}_s \mathbf{w}_t - 2H w_n = \operatorname{div}_s \mathbf{w} . \tag{A.2.16}$$

Now we return to (A.2.14) which becomes

$$\frac{d}{dt} \int_{\Sigma'(t)} \psi' \, dS = \int_{\Sigma'(t)} \left(\frac{d_s \psi'}{dt} + \psi' \operatorname{div}_s \mathbf{w} \right) dS \tag{A.2.17}$$

or, thanks to the definition of the material derivative (2.25) and an obvious identity,

$$\text{(A.2.18)}\quad \frac{d}{dt}\int_{\Sigma'(t)} \psi'\, dS = \int_{\Sigma'(t)} \left(\left.\frac{\partial \psi'}{\partial t}\right|_{\tilde{y}^\beta} + \nabla_s \psi' \cdot w_t + \operatorname{div}_s(\psi' \mathbf{w}) - \nabla_s \psi' \cdot w \right) dS$$

$$= \int_{\Sigma'(t)} \left(\left.\frac{\partial \psi'}{\partial t}\right|_{\tilde{y}^\beta} - \nabla_s \psi' \cdot W_N + \operatorname{div}_s(\psi' \mathbf{w}) \right) dS .$$

The last term in (A.2.18) may be replaced according to (A.2.16) by

$$\text{(A.2.19)}\qquad \operatorname{div}_s(\psi' \mathbf{w}) = \operatorname{div}_s(\psi' \mathbf{w}_t) - 2H\psi' w_n .$$

Since $\Sigma'(t)$ is a regular subsurface, its boundary $\partial\Sigma'(t)$ is piecewise smooth and the surface divergence theorem (GURTIN, MURDOCH [19]) gives

$$\text{(A.2.20)}\qquad \int_{\Sigma'(t)} \operatorname{div}_s(\psi' \mathbf{w}_t)\, dS = \int_{\partial\Sigma'(t)} \psi' \mathbf{w}_t \cdot m\, dl ,$$

where $\mathbf{m}$ is the outward unit surface vector normal to the bounding curve $\partial\Sigma'(t)$ at M and belonging to the tangent plane of $\Sigma'(t)$ at $\partial\Sigma'(t)$. An alternative form of (A.2.17) is then

$$\text{(A.2.21)}\quad \frac{d}{dt}\int_{\Sigma'(t)} \psi'\, dS = \int_{\Sigma'(t)} \left(\left.\frac{\partial \psi'}{\partial t}\right|_{\tilde{y}^\beta} - \nabla_s \psi' \cdot w_n - 2H\psi' w_n \right) dS$$

$$+ \int_{\partial\Sigma'(t)} \psi' \mathbf{w}_t \cdot m\, dl .$$

Appendix 3. Numerical techniques

In this appendix, numerical approximations of the system (6.8), (6.10) (or (6.24) and (6.26)) are presented. Let us first consider the Fredholm integral equation (6.10). Numerical solutions of such integral equations have been used first by HESS and SMITH [20], who appeared as the pioneers of that matter in potential flows. Usually, the numerical procedure uses a spatial discretization of both surface and singularity distributions according to a very simple approach: the surface is represented by N flat elements (straight-line segments in our axisymmetric applications) on which the density of the singularity distribution is constant. So, the Fredholm integral equation is approximated by a linear set of equations of order N. At each time step, our problem (defined in Sect. 6) is entirely determined by

(i) the position of N markers in an arbitrary meridian plane,

$$\text{(A.3.1)}\qquad M_i(r_i, z_i), \quad i = 1, N ;$$

(ii) the values of the surface potential defined in (6.9)

$$\text{(A.3.2)}\qquad \Phi_i(M_i), \quad i = 1, N .$$

Then, the N unknowns are the densities τ_i, which are the solutions of the system

$$\text{(A.3.3)}\qquad \Phi_i = \tau_i - 2A \sum_{j=1}^{N} G_{ij} \tau_j, \quad i = 1, N ,$$

where

$$G_{ij} = \int_{S_j} \frac{\partial G}{\partial n}(M_i, s)\, dS, \quad i, j = 1, N. \tag{A.3.4}$$

In this linear reformulation, M_i is the collocation point located at the center of the segment S_i. In practice, the G_{ij} terms, called influence coefficients, are evaluated analytically and numerically (see, e.g. HESS and SMITH [20], BLAKE *et al.* [9]. The linear system obtained from (A.3.3)

$$A_{ij}\tau_j = \Phi_i, \quad i, j = 1, N \tag{A.3.5}$$

is solved in our case by a standard Gaussian elimination (see HESS and SMITH [20], or BMO [4], for iterative methods). Once the values of τ_j are obtained, the velocities on S are computed by taking into account the equivalence between the dipole and the vortex representation. The velocity field $\mathbf{v}$ defined by Eq. (4.30) is derived in our case from N vortex rings intensities

$$\gamma_i = \tau_i - \tau_{i+1}, \quad i = 1, N \tag{A.3.6}$$

which bound the segments S_i.

Then, we are able to update the position of each marker M_i and the potentials Φ_i by using a simple first order scheme

$$M_i(t + \Delta t) \begin{cases} r_i(t + \Delta t) = r_i(t) + u_i \Delta t, \\ z_i(t + \Delta t) = z_i(t) + \nu_i \Delta t, \end{cases} \quad i = 1, N, \tag{A.3.7}$$

where (u_i, ν_i) are the (r, z) components of the normal velocity of the surface, and

$$\Phi_i[M_i(t + \Delta t)] = \Phi_i[M_i(t)] + \left(\frac{d_s\Phi}{dt}\right)_i \Delta t, \quad i = 1, N, \tag{A.3.8}$$

where $d_s\Phi/dt$ is computed by Eq. (6.8). At this point, a new mesh of $S(t + \Delta t)$ is generated by the procedure described in Appendix 1, furnishing N' new points M_i'. Note that, in general, N' is not equal to N, and increases as the shape of S becomes more and more complicated. The values of r, z, Φ at this new point are obtained by a cubic-spline smoothing technique (MARCHOUK [30]). We must point out here that this smoothing is required in order to remove non-physical irregularities, developing a saw-toothed appearance, due to the crudeness of the schemes used (see LONGUET–HIGGINS and COKELET [28]), and also in order to avoid too small time-steps. The choice of Δt at each time step is based on the limitation of the normal deformation of the interface.

High order schemes would be envisaged for the numerical approximation presented above. For the spatial discretization (A.3.4) see for example BREBBIA et al. [11]. For the time stepping procedure refer to BMO [3,4], PULLIN [41], TELSTE [49], LUNGREN and MANSOUR [29]. Another interesting technique would probably be the use of an efficient time-stepping procedure established by DOLD and PEREGRINE [17] which attain great accuracy via the calculation of multiple time-derivatives.

Acknowledgement

The authors wish to thank the "Direction des Recherches, Etudes et Technique du Ministère de la Défense" for their financial support.

References

1. R. ARIS, *Vectors, tensors and basic equations of fluid mechanics*, Prentice-Hall, Englewood Cliffs, New York 1962.
2. G. R. BAKER, *A test of the method of Fink and Soh for following vortex-sheet motion*, J. Fluid Mech., **100**, 1, pp. 209-220, 1980.
3. G. R. BAKER, D. I. MEIRON and S. A. ORSZAG, *Vortex simulations of the Rayleigh-Taylor instability*, Phys. Fluids, **23**, 8, 1485-1490, 1980.
4. G. R. BAKER, D.I. MEIRON and S. A. ORSZAG, *Generalized vortex methods for free-surface flow problems*, J. Fluid Mech., **123**, 477-501, 1982.
5. G. R. BAKER, D. I. MEIRON and S. A. ORSZAG, *Boundary integral methods for axisymmetric and three-dimensional Rayleigh-Taylor instability problems*, Physica, D **12**, 19–31, 1984.
6. C. T. H. BAKER and G. F. MILLER, *Treatment of integral equations by numerical methods*, Symposium of Durham, Academic Press, 1982.
7. G. BIRKHOFF, *Helmoltz and Taylor instability*, Proc. Symp. Appl. Math., **13**, Amer. Math. Soc., Providence, RI, 1962.
8. J. R. BLAKE and D. C. GIBSON, *Growth and collapse of a vapour cavity near a free surface*, J. Fluid Mech., **111**, 123–140, 1981.
9. J. R. BLAKE, B. B. TAIB and G. DOHERTY, *Transient cavities near boundaries. Part I. Rigid boundary*, J. Fluid Mech., **170**, 479–497, 1986.
10. R. M. BOWEN and C. C. WANG, *Introduction to vectors and tensors. 1. Linear and multilinear algebra. 2. Vector and tensor analysis*, Plenum Press, New York, London 1976.
11. C. A. BREBBIA, J. C. F. TELLES and L. C. WROBEL, *Boundary element techniques. Theory and applications in engineering*, Springer-Verlag, Berlin and New-York 1984.
12. M. CESCHIA and R. NABERGOJ, *On the motion of a nearly spherical bubble in a viscous liquid*, Phys. Fluids, **21**, 1, 140–142, 1978.
13. S. CHANDRASEKHAR, *Hydrodynamic and hydromagnetic stability*, Oxford University Press, London 1961.
14. B. J. DALY, *Numerical study of the effect of surface tension on interface instability*, Phys. Fluids, **12**, 7, 1340–1354, 1969.
15. A. R. DEEMER and J. C. SLATTERY, *Balance equations and structural models for phase interfaces*, Int. J. Multiphase Flow, **4**, 171–192, 1978.
16. J. M. DELHAYE, *Jump conditions and entropy sources in two-phase systems. Local instant formulation*, Int. J. Multiphase Flow, **1**, 395–409, 1974.
17. J. W. DOLD and D. H. PEREGRINE, *An efficient boundary-integral method for steep unsteady water waves*, Numerical Methods for Fluid Dynamics II, Eds. K. W. Morton and M. J. Baines, Clarendon, pp. 671–679, 1986.
18. P. T. FINK and W. K. SOH, *A new approach to roll-up calculation of vortex sheets*, Proc. Soc. Lond., A 362, pp. 195–209, 1978.
19. M. E. GURTIN and A. I. MURDOCH, *A continuum theory of elastic material surfaces*, Arch. Rat. Mech. Anal., **57**, pp. 291–323, 1975.
20. J. L. HESS and A. M. O. SMITH, *Calculation of potential flow about arbitrary bodies*, Progr. in Aero. Sci., **8**, Pergamon Press, London 1967.
21. M. A. JASWON and G. T. SYMM, *Integral equation methods in potential theory*, Academic Press, New York and London 1977.
22. I. S. KANG and L. G. LEAL, *The drag coefficient for a spherical bubble in a uniform streaming flow*, Phys. Fluids, **31**, 2, pp. 233–237, 1988.
23. R. M. KERR, *Simulation of Rayleigh-Taylor flows using vortex blobs*, J. Comput. Phys., **76**, 48–84, 1988.
24. R KRASNY, *Desingularization of periodic vortex sheet roll-up*, J. Comput. Phys., **65**, 292–313, 1986.
25. H. LAMB, *Hydrodynamics*, University Press, Cambridge 1932.
26. M. LENOIR, *Simulation numérique du "collapse" d'une bulle de cavitation*, Rapport de recherche 064, ENSTA, Fév. 1976.
27. D. L. LEWIS, *The instability of liquid surfaces when accelerated in a direction perpendicular to their planes. Part II*, Proc. Roy. Soc. Lond., **A 202**, pp. 81–96, 1950.
28. M. S. LONGUET-HIGGINS and E. D. COKELET, *The deformation of steep surface waves on water. I. A numerical method of computation*, Proc. Roy. Soc. London, **A 350**, pp. 1–26, 1976.

29. T. S. LUNDGREN and N. N. MANSOUR, *Oscillations of drops in zero gravity with weak viscous effects*, J. Fluid Mech., **194**, pp. 479–510, 1988.
30. A. MARCHOUK, *Méthodes de calcul numérique*, Editions Mir, 1980.
31. D. I. MEIRON, G. R. BAKER and S. A. ORSZAG, *Analytic structure of vortex sheet dynamics. Part. I. Kelvin-Helmholtz instability*, J. Fluid Mech., **114**, pp. 283–298, 1982.
32. R. MENIKOFF and C. ZEMACH, *Rayleigh-Taylor instability and the use of conformal maps for ideal fluid flow*, J. Comput. Phys., **51**, 28–64, 1983.
33. M. J. MIKSIS, J. M. VANDEN-BROECK and J. B. KELLER, *Rising bubbles*, J. Fluid Mech., **123**, 31–41, 1982.
34. T. M. MITCHELL and F. G. HAMMITT, *Asymptotic cavitation bubble collapse*, J. Fluids Engng. ASME Trans., pp. 29–36, March 1973.
35. D. W. MOORE, *The rise of a gas bubble in a viscous liquid*, J. Fluid Mech., **6**, 113–130, 1959.
36. D. W. MOORE, *The boundary layer on a spherical gas bubble*, J. Fluid Mech., **16**, 161–176, 1963.
37. D. W. MOORE, *The spontaneous appearance of a singularity in the shape of an evolving vortex sheet*, Proc. Roy. Soc. London, **A 365**, 105–119, 1979.
38. M. S. PLESSET and R. B. CHAPMAN, *Collapse of an initially spherical vapour cavity in the neighbourhood of a solid boundary*, J. Fluid Mech., **47**, 2, 283–290, 1971.
39. A. PROSPERETTI, *Bubbles dynamics: a review and some recent results*, Appl. Sci. Res., **38**, 145–164, 1982.
40. A. PROSPERETTI and J. W. JACOBS, *A numerical method for potential flows with a free surface*, J. Comput. Phys., **51**, 365–386, 1983.
41. D. I. PULLIN, *Numerical studies of surface-tension effects in non-linear Kelvin-Helmholtz and Rayleigh-Taylor instability*, J. Fluid Mech., **119**, 507–532, 1982.
42. R. H. RANGEL and W. A. SIRIGNANO, *Nonlinear growth of Kelvin-Helmholtz instability: effects of surface tension and density ratio*, Phys. Fluids, **31**, 7, 1845–1855, 1988.
43. A. J. ROBERTS, *A stable and accurate numerical method to calculate the motion of a sharp interface between fluids*, IMA J. Appl. Math., **31**, 13–35, 1983.
44. L. ROSENHEAD, *The formation of vortices from a surface of discontinuity*, Proc. Roy. Soc. London, **A 134**, 170-192, 1931.
45. L. SEDOV, *Mécanique des milieux continus*, T. 2, MIR, 1975.
46. J. C. SLATTERY and R. W. FLUMERFELT, *Interfacial phenomena*, in: Handbook of Multiphase Systems, Ed. G. Mestroni, Hemisphere and Mc Graw-Hill, **1.4**, pp. 1.224-1.254, 1982.
47. I. STAKGOLD, *Green's functions and boundary value problems*, Wiley, 1979.
48. G. I. TAYLOR, *The instability of liquid surfaces when accelerated in a direction perpendicular to their planes. Part I.*, Proc. Roy. Soc. London, **A 201**, 192-196, 1950.
49. J. G. TELSTE, *Inviscid flow about a cylinder rising to a free surface*, J. Fluid Mech., **182**, 149–168, 1987.
50. J. F. THOMPSON, Z. U. A. WARSI and C. W. MASTIN, *Boundary fitted coordinate systems for numerical solution of partial differential equations. A review*, J. Comput. Phys., **47**, 1–108, 1982.
51. G. TRYGGVASON, *Deformation of a free surface as a result of vortical flows*, Phys. Fluids, **31**, **5**, 955–957, 1988.
52. C. S. YIH, *Dynamics of non-homogeneous fluids*, McMillan Company, New York 1965.
53. J. A. ZUFIRIA, *Vortex-in-cell simulation of bubble competition in a Rayleigh-Taylor instability*, Phys. Fluids, **31**, 11, 3199–3212, 1988.

INSTITUT DE MECANIQUE DE GRENOBLE, GRENOBLE, FRANCE.

Received January 7, 1991.